
Achieving robustness in classification using optimal transport with hinge regularization

Mathieu Serrurier

IRIT

Université Paul Sabatier Toulouse

Franck Mamalet

IRT Saint-Exupéry

Alberto González-Sanz

IMT

Université Paul Sabatier Toulouse

Thibaut Boissin

IRT Saint-Exupéry

Jean-Michel Loubes

IMT

Université Paul Sabatier Toulouse

Eustasio del Barrio

Dpto. de Estadística e Investigación Operativa

Universidad de Valladolid

Abstract

We propose a new framework for robust binary classification, with Deep Neural Networks, based on a hinge regularization of the Kantorovich-Rubinstein dual formulation for the estimation of the Wasserstein distance. The robustness of the approach is guaranteed by the strict Lipschitz constraint on functions required by the optimization problem and direct interpretation of the loss in terms of adversarial robustness. We prove that this classification formulation has a solution, and is still the dual formulation of an optimal transportation problem. We also establish the geometrical properties of this optimal solution. We summarize state-of-the-art methods to enforce Lipschitz constraints on neural networks and we propose new ones for convolutional networks (associated with an open source library for this purpose). The experiments show that the approach provides the expected guarantees in terms of robustness without any significant accuracy drop. The results also suggest that adversarial attacks on the proposed models visibly and meaningfully change the input, and can thus serve as an explanation for the classification.

1 Introduction

The important progress in deep learning has led to a massive interest for these approaches in industry. However, when machine learning is applied for critical tasks such as in the transportation or the medical domain, empirical and theoretical guarantees are required. Some recent papers [7] propose theoretical guarantees for particular neural networks, but this remains an open problem for Deep Neural Networks. Empirically, weakness of deep models with respect to adversarial attack was first shown in [27], and is an active research topic. [27] pointed out that sensitivity to adversarial attack is closely related to the high Lipschitz constant of an unconstrained deep classifier. Defense methods relying on Lipschitz constraints have also been proposed [6; 16; 21; 22]. Moreover it has been proven that limiting the Lipschitz constant improves generalisation [26] and the interpretability of the model [29], i.e. higher sparsity and interpretability. Counterfactual explanation in machine learning considers what we have to change in a situation to change the prediction [32]. For models based on high-level language such as logic, this modification is interpretable as itself and provides an explanation of the prediction. It turns out that, for neural networks, the definition of counterfactual corresponds exactly to adversarial attacks, but these are usually indistinguishable from noise.

k -Lipschitz networks have also been used in Wasserstein GAN [2] to measure the distance between two distributions as a discriminator, in analogy with the initial GAN algorithm [12]. The Wasserstein distance is approximated using a loss based on the Kantorovich-Rubinstein dual formulation and a k -Lipschitz network constrained by weight clipping. An interesting property of this approach, but not harnessed in WGAN, is the link with optimal transportation that provides a nice interpretation of the loss function in terms of robustness. However, we will show that a vanilla classifier based on the Kantorovich-Rubinstein problem is suboptimal, even on toy datasets.

In this paper, we propose a binary classifier based on a regularized version of the dual formulation of the Wasserstein distance, combining the Kantorovich-Rubinstein loss function with a hinge loss. With this new optimization problem, we ensure to have an accurate classifier with a loss that has a direct interpretation in terms of robustness due to the 1-Lipschitz constraint. Moreover, we show that it is still the dual of an optimal transportation problem. We prove that the optimal solution of the problem exists and makes no error when the classes are well separated. Our approach shares some similarities with Parseval networks [6], in the way we constraint the Lipschitz constant of the networks by spectral normalization and orthonormalization of the weights. However, the new loss function we propose takes a better advantage of the Lipschitz constant limitation. The geometric properties of the optimal solution of our problem encourage us to consider more advanced regularization techniques proposed in [1] such as Björck normalization and a gradient preserving activation function. Experimentation shows that the proposed approach matches the state-of-the-art in terms of accuracy and demonstrates higher robustness to adversarial attacks. We also emphasizes that the classifier output has a direct interpretation in terms of robustness. Last, we show that adversarial examples for our classifier perform input changes that are interpretable, and thus are close to the notion of counterfactuals.

The paper, and the contributions, are structured as follows. In Section 2, we recall the definition of Wasserstein distance and the dual optimization problem associated. We present the interesting properties of a classifier based on this approach and we illustrate that it leads to a suboptimal classifier. Section 3 describes the proposed binary classifier, based on a regularized version of the Kantorovich-Rubinstein loss with a hinge loss. We show that the primal of this classification problem is a new optimal transport problem and we demonstrate different properties of our approach. Section 4 is devoted to the way of constraining the classifier to be 1-Lipschitz. We recall the different approaches to performs Lipschitz regularization, and also propose a new way to consider the regularization for convolutional and pooling layers. Section 5 presents the results of experiments on MNIST and CelebA datasets, measuring and comparing the results of different approaches in terms of accuracy and robustness. It also illustrates that the 1-Lipschitz constraint is satisfied. Last, we demonstrate that with our approach, building an adversarial example requires explicitly changing the example to an in-between two-classes image. We also show that we can easily build a counterfactual example, based the gradient of our network on the considered point, that can be used as an explanation for a classification. Proofs, computations details and additional experiments are reported in the appendix.

2 Wasserstein distance and Kantorovich-Rubinstein classifier

In this paper we only consider the Wasserstein-1 distance, also called Earth-mover, and noted \mathcal{W} for \mathcal{W}_1 . The 1-Wasserstein distance between two probability distributions μ and ν in Ω , and its dual formulation by Kantorovich-Rubinstein duality [30], is defined as the solution of:

$$\mathcal{W}(\mu, \nu) = \inf_{\pi \in \Pi(\mu, \nu)} \mathbb{E}_{x, z \sim \pi} \| \mathbf{x} - \mathbf{z} \| \quad (1a)$$

$$= \sup_{f \in Lip_1(\Omega)} \mathbb{E}_{\mathbf{x} \sim \mu} [f(\mathbf{x})] - \mathbb{E}_{\mathbf{x} \sim \nu} [f(\mathbf{x})] \quad (1b)$$

where $\Pi(\mu, \nu)$ is the set of all probability measures on $\Omega \times \Omega$ with marginals μ and ν and $Lip_1(\Omega)$ denotes the space of 1-Lipschitz functions over Ω . Although, the infimum in Eq. (1a) is not tractable in general, the dual problem can be estimated through the optimization of a regularized neural network. This approach has been introduced in WGAN [2] where $Lip_1(\Omega)$ is approximated by the set of neural networks with bounded weights (better approaches to achieve it will be discussed in Section 4).

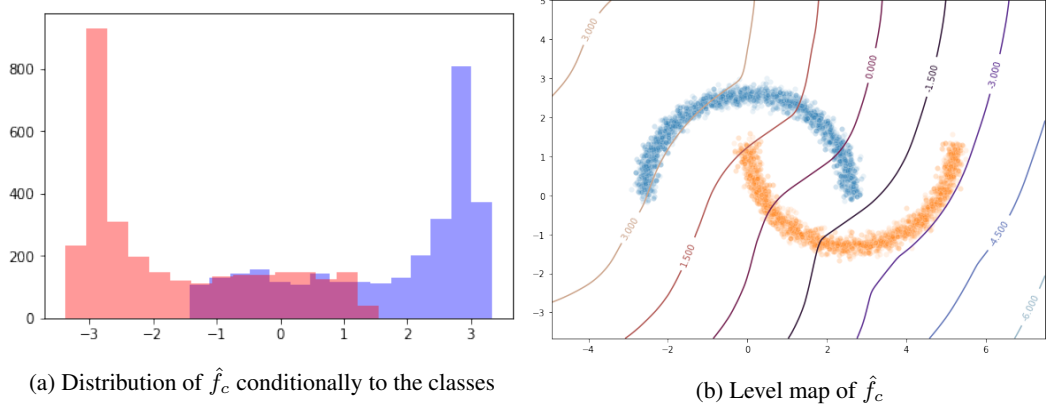


Figure 1: Wasserstein classification (Eq. (2)) on the two moons.

We consider a binary classification problem on feature vector space $X \subset \Omega$ and labels $Y = \{-1, 1\}$. We name $P_+ = \mathbb{P}(X|Y = 1)$ and $P_- = \mathbb{P}(X|Y = -1)$, the conditional distributions with respect to Y . We note $p = P(Y = 1)$ and $1 - p = P(Y = -1)$ the apriori class distribution. The classification problem is balanced when $p = \frac{1}{2}$.

In WGAN, [2] proposed to use the learned neural network (denoted \hat{f} in the following), by maximizing the Eq. (1b), as a discriminator between fake and real images, in analogy with GAN [12]. To build a classifier based on \hat{f} , one can simply note that if f^* is an optimal solution of Eq. (1b), then $f^* + C, C \in \mathbb{R}$, is also optimal. Centering the function f^* (resp. \hat{f}), Eq. (2), enables classification according to the sign of $f_c^*(x)$ (resp. \hat{f}_c for the empirical solution).

$$f_c^*(\mathbf{x}) = f^*(\mathbf{x}) - \frac{1}{2} \left(\mathbb{E}_{\mathbf{z} \sim P_+} [f^*(\mathbf{z})] + \mathbb{E}_{\mathbf{z} \sim P_-} [f^*(\mathbf{z})] \right). \quad (2)$$

Such a classifier would exhibit good properties in terms of robustness for two main reasons: First, it has been shown in [30] that the function f^* is directly related to the cost of transportation between two points linked by the transportation plan (when $\pi^*(x = y) = 0$) as follows:

$$\mathbb{P}_{\mathbf{x}, \mathbf{z} \sim \pi^*} (f^*(\mathbf{x}) - f^*(\mathbf{z})) = \|\mathbf{x} - \mathbf{z}\| = 1. \quad (3)$$

Second, it was shown in [13; 1], that this optimal solution also induces a property stronger than 1-Lipschitz:

$$\|\nabla f^*\| = 1 \text{ almost surely on the support of } \pi^*. \quad (4)$$

However, applying this vanilla classifier (Eq. (2)) to a toy dataset such as the two-moons problem, leads to a poor accuracy. Indeed, Figures 1a and 1b present respectively the distribution of the values of $\hat{f}_c(x)$ conditionally to the classes and the level map of \hat{f}_c . We can observe that, even if the classes are easily separable, the distributions of the values of \hat{f}_c conditionally to the class overlap. Thus, the 0-level threshold on \hat{f}_c does not correspond to the optimal separator (even if it is better than random). Intuitively, \hat{f}_c maximizes the difference of the expectancy of the image of the two distributions but do not try to minimize their overlap (Fig. 1a).

3 Hinge regularized Kantorovich-Rubinstein classifier

3.1 Definitions and primal transportation problem

In order to improve the classification abilities of the classifier based on Wasserstein distance, we propose a Kantorovich-Rubinstein optimization problem regularized by an hinge loss :

$$\sup_{f \in Lip_1(\Omega)} -\mathcal{L}_\lambda^{hKR}(f) = \sup_{f \in Lip_1(\Omega)} - \left(\mathbb{E}_{\mathbf{x} \sim P_-} [f(\mathbf{x})] - \mathbb{E}_{\mathbf{x} \sim P_+} [f(\mathbf{x})] + \lambda \mathbb{E}_{\mathbf{x}} (1 - Y f(\mathbf{x}))_+ \right) \quad (5)$$

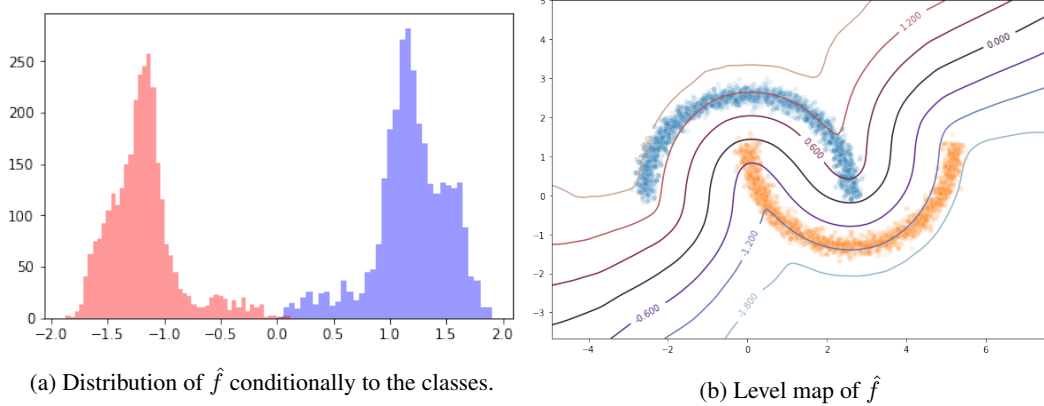


Figure 2: Hinge regularized Kantorovich-Rubinstein (hinge-KR) classification on the two moons problem

where $(1 - \mathbf{y}f(\mathbf{x}))_+$ stands for the hinge loss $\max(0, 1 - \mathbf{y}f(\mathbf{x}))$ and $\lambda \geq 0$. We name $\mathcal{L}_\lambda^{hKR}$ the hinge-KR loss. The goal is then to minimize this loss with an 1-Lipschitz neural network.

When $\lambda = 0$, this corresponds to the Kantorovich-Rubinstein dual optimization problem. Intuitively, the 1-Lipschitz function f^* optimal with respect to Eq. (5) is the one that both separates the examples with a margin and spreads as much as possible the image of the distributions.

In the following, we introduce Theorems that prove the existence of such an optimal function f^* and important properties of this function. Demonstrations of these theorems are in Appendix B.

Theorem 1 (Solution existence). *For each $\lambda > 0$ there exists at least a solution f^* to the problem*

$$f^* := f_\lambda^* \in \arg \min_{f \in Lip_1(\Omega)} \mathcal{L}_\lambda^{hKR}(f).$$

Moreover, let ψ be an optimal transport potential for the transport problem from P_+ to P_- , f^* satisfies that

$$\|f^*\|_\infty \leq M := 1 + \text{diam}(\Omega) + \frac{L_1(\psi)}{\inf(p, 1-p)}. \quad (6)$$

The next theorem establishes that the Kantorovich-Rubinstein optimization problem with hinge regularization is still a transportation problem with relaxed constraints on the joint measure (which is no longer a joint probability measure).

Theorem 2 (Duality). *Set $P_+, P_- \in \mathcal{P}(\Omega)$ and $\lambda > 0$, then the following equality holds*

$$\sup_{f \in Lip_1(\Omega)} -\mathcal{L}_\lambda^{hKR}(f) = \inf_{\pi \in \Pi_\lambda^p(P_+, P_-)} \int_{\Omega \times \Omega} |\mathbf{x} - \mathbf{z}| d\pi + \pi_x(\Omega) + \pi_z(\Omega) - 1 \quad (7)$$

Where $\Pi_\lambda^p(P_+, P_-)$ is the set consisting of positive measures $\pi \in \mathcal{M}_+(\Omega \times \Omega)$ which are absolutely continuous with respect to the joint measure $dP_+ \times dP_-$ and $\frac{d\pi_x}{dP_+} \in [p, p(1 + \lambda)]$, $\frac{d\pi_z}{dP_-} \in [1 - p, (1 - p)(1 + \lambda)]$.

3.2 Classification and geometrical properties

We note \hat{f} the solution obtained by minimizing $\mathcal{L}_\lambda^{hKR}$ on a set of labeled examples and f^* the solution of Eq. (5). We don't assume that the solution found is optimal (i.e. $\hat{f} \neq f^*$) but we assume that \hat{f} is 1-Lipschitz. Given a function f , a classifier based on $sign(f)$ and an example x , an adversarial example is defined as follows:

$$adv(f, \mathbf{x}) = \underset{\mathbf{z} \in \Omega | sign(f(\mathbf{z})) = -sign(f(\mathbf{x}))}{\text{argmin}} \|\mathbf{x} - \mathbf{z}\|. \quad (8)$$

According to the 1-Lipschitz property of \hat{f} we have

$$|\hat{f}(\mathbf{x})| \leq |\hat{f}(\mathbf{x}) - \hat{f}(adv(\hat{f}, \mathbf{x}))| \leq \|\mathbf{x} - adv(\hat{f}, \mathbf{x})\|. \quad (9)$$

So $|\hat{f}(\mathbf{x})|$ is a lower bound of the distance of x to the separating boundary defined by \hat{f} and thus a lower bound to the robustness to l_2 adversarial attacks. By minimizing $\mathbb{E}((1 - \mathbf{y}f(\mathbf{x}))_+)$, we maximize the accuracy of the classifier and by maximizing the discrepancy of the image of P_+ and P_- with respect to f we maximize the robustness with respect to adversarial attack. The proposition below establishes that the gradient of the optimal function with respect to Eq. (5) has norm 1 almost surely, as for the unregularized case (Eq. (4)).

Proposition 1. *Let π be the optimal measure of the dual version (7) of the hinge regularized optimal transport problem. Suppose that it is absolutely continuous with respect to Lebesgue measure. Then there exists at least a solution f^* of (7) such that $\|\nabla f^*\| = 1$ almost surely.*

Furthermore, empirical results suggest that given \mathbf{x} , the image $tr_{f^*}(\mathbf{x})$ of \mathbf{x} with respect to the transportation plan and $adv(\mathbf{x})$ are in the same direction with respect to \mathbf{x} and the direction is $-\nabla_x f^*(\mathbf{x})$. Combining this direction with the Eq. (9), we will show empirically (sect. 5) that

$$adv(\mathbf{x}) \approx x - c_x * f^*(\mathbf{x}) * \nabla_x f^*(\mathbf{x})$$

and

$$tr_{f^*}(\mathbf{x}) \approx x - c'_x * f^*(\mathbf{x}) * \nabla_x f^*(\mathbf{x})$$

with $1 \leq c_x \leq c'_x \in \mathbb{R}$. This provides a strong link between the adversarial attack and the optimal transport for the proposed classifier.

The next proposition shows that, if the classes are well separated, maximizing the hinge-KR loss leads to a perfect classifier.

Proposition 2 (Separable classes). *Set $P_+, P_- \in \mathcal{P}(\Omega)$ such that $P(Y = +1) = P(Y = -1)$ and $\lambda \geq 0$ and suppose that there exists $\epsilon > 0$ such that*

$$|\mathbf{x} - \mathbf{z}| > 2\epsilon \text{ } dP_+ \times dP_- \text{ almost surely} \quad (10)$$

Then for each

$$f_\lambda \in \arg \sup_{f \in Lip_{1/\epsilon}(\Omega)} \int_{\Omega} f(dP_+ - dP_-) - \lambda \left(\int_{\Omega} (1 - f)_+ dP_+ + \int_{\Omega} (1 + f)_+ dP_- \right), \quad (11)$$

it is satisfied that $L_1(f_\lambda) = 0$. Furthermore if $\epsilon \geq 1$ then f_λ is an optimal transport potential from P_+ to P_- for the cost $|\mathbf{x} - \mathbf{z}|$.

We show in Fig. 2, on the two moons problem, that in contrast to the vanilla classifier based on Wasserstein (Eq. (2)), the proposed approach enables non overlapping distributions of \hat{f} conditionally to the classes (Fig. 2a). In the same way, the 0-level cut of \hat{f} (Fig. 2b) is a nearly optimal classification boundary. Moreover, the level cut of \hat{f} , on the support of the distributions, is close to the distance to this classification boundary.

4 1-Lipschitz neural networks

In order to build a deep learning classifier based on the hinge-KR optimization problem (Eq. (5)), we have to constrain the Lipschitz constant of the neural network to be equal to 1. Even if the control of the Lipschitz constant of a neural network is a key step to guarantee some robustness [6], it is known that evaluating it exactly is a np-hard problem [31]. The simplest strategy is to constraint each layer of the network to be 1-Lipschitz, to ensure that the Lipschitz constant of composition of the functions will be less than or equal to one. Most common activation functions such as ReLU or sigmoid are 1-Lipschitz. In the case of a dense layer, constraints can be applied to its weights. The simplest strategy is to constraint the weights of each layer. Given a dense layer with weights W , It is commonly admitted that:

$$L(W) = \|W\| \leq \|W\|_F \leq \max_{ij}(|W_{ij}|) * \sqrt{nm} \quad (12)$$

where $\|W\|$ is the spectral norm, and $\|W\|_F$ is the Frobenius norm. The initial version of WGAN [2] consisted of clipping the weights of the networks. However, this is a very crude way to upper-bound Lipschitz constant (last term in Eq. (12)). Normalizing by the Frobenius norm has also been proposed in [25]. In this paper, we use spectral normalization as proposed in [19], since

the spectral norm is equals to the Lipschitz constant. At the inference step, we normalize the weights of each layer by dividing the weights by the spectral norm of the matrix. The spectral norm is computed by iteratively evaluating the largest singular value with the power iteration algorithm [11]. This is done during the forward step and taken into account for the gradient computation.

In the case of 2D-convolutional layers, normalizing by the spectral norm of the convolution kernels is not enough and a supplementary multiplicative constant Λ is required (the regularization is then done by dividing W by $\Lambda ||W||$). Given a convolutional layer with a kernel size equals to $k = 2 * \bar{k} + 1$, the coefficient Λ can be estimated, as in [6], as the square root of the maximum number of duplications of the input matrix values: since each input can be used in at most k^2 positions, choosing $\Lambda = k$ guarantees the convolutional layers to be 1-Lipschitz. However, due to the effect of the zero-padding, the constant Λ is overestimated and the real Lipschitz constant is lower than 1, especially when the size of the image is small. When the convolutional network is very deep, this heavily decreases the Lipschitz constant of the neural network. To mitigate this effect, we propose, for zero padding, a tighter estimation of Λ , computing the average duplication factor of non zero padded values in the feature map:

$$\Lambda = \sqrt{\frac{(k.w - \bar{k}.(\bar{k} + 1)).(k.h - \bar{k}.(\bar{k} + 1))}{h.w}}. \quad (13)$$

Even if this constant doesn't provide a strict upper bound of the Lipschitz constant (for instance, when the higher values are located in the center of the picture), it behaves very well empirically (see Figure 3b for instance). Convolution with stride, pooling layers, detailed explanations and demonstrations are discussed in Appendix C.3.

As shown in Section 3.2, the optimal function f^* with respect to Eq. (5), verifies $||\nabla f^*|| = 1$ almost surely. In [13], the authors propose to add a regularization term with respect to the average gradient norm with respect to inputs in the loss function. However, the estimation of this value is difficult and a regularization term doesn't guarantee the property. In this paper, we apply the approach described in [1], based on the use of specific activation functions and a process of normalization of the weights. Two norm preserving activation functions are proposed: i) **GroupSort2** : order the vector by pairs, ii) **FullSort** : order the full vector. These functions are vector-wise rather than element-wise. We also use the P-norm pooling [4], with $P = 2$ which is a norm-preserving average pooling. Concerning linear functions, a weight matrix W is norm preserving if and only if all the singular values of W are equals to 1. In [1], the authors propose to use the Bjrk orthonormalization algorithm [3]. This algorithm is fully differential and, as for spectral normalization, is applied during the forward inference, and taken into account for back-propagation (see Appendix C.4 for details). We also developed a full tensorflow [8] implementation in an opensource library, called *DEEL.LIP*¹, that enables training of k-Lipschitz neural networks, and exporting them as standard layers for inference.

5 Experiments

In the experiment, we compare three different approaches: i) classical log-entropy classifier (MLP/CNN), ii) 1-Lipschitz log-entropy classifier (1LIP-MLP/1LIP-CNN), in the spirit of Parseval networks, iii) hinge-KR classifier (hKR-MLP/hKR-CNN). In order to have a fair comparison, all the classifiers share the same dense or convolutional architecture. For the 1-Lipschitz log-entropy, we perform spectral normalization within the experiments with 3 power iteration steps and we use ReLU activation (gradient preserving activations and pooling make no sense in this case and Bjrk orthonormalization doesn't improve the results). For the hinge-KR classifiers, we apply Bjrk orthonormalization (15 steps with $p=1$) after the spectral normalization (this improves the convergence of the Bjrk algorithm). We use fullsort activation for dense layers and GroupSort2 for the convolutional ones. The full description of the architecture, the optimization process, and the influence of each parameter are described in Appendix D.1.

For adversarial robustness estimation, since the hinge-KR primal problem is linked to L_2 distance, we focus on L_2 based adversarial attacks using the *DeepFool* framework [20]. For each type of Neural Network, 500 attacks are carried out on test sets (using the *foolbox* library [23]), storing

¹<https://github.com/deel-ai/deel-lip> to be published soon

Dataset	Network archi	loss	Accuracy	Attack Robustness
MNIST 0-8	<i>MLP</i>	bin_cross.	99.6	4.47
	<i>1LIP – MLP</i>	bin_cross.	99.5	6.29
	<i>hKR – MLP</i>	$L_\lambda^{hKR} (\lambda = 10)$	99.0	7.19
	<i>hKR – MLP</i>	$L_\lambda^{hKR} (\lambda = 50)$	99.2	7.36
Celeb-A Moustache	<i>CNN</i>	bin_cross.	92.6	0.45
	<i>1LIP – CNN</i>	bin_cross.	92.4	0.27
	<i>hKR – CNN</i>	$L_\lambda^{hKR} (\lambda = 20)$	90.9	3.87

Table 1: Accuracy and robustness to adversarial attack (average noise L_2 norm) comparison

for each image the *output* value, and the L_2 norm of noise required to fool the network (up to a 50/50 score). The *output* value is either the last dense layer output before the sigmoid activation for MLP/CNN and 1LIP-MLP/1LIP-CNN networks (commonly called *logit* layer), or the last layer output for the hKR-MLP/hKR-CNN classifier. We consider two binary classification problems. The first one is the separation of the digits 0 and 8 on the MNIST dataset (balanced classes, 10596 training, and 1954 test samples). We choose these particular pair of digits because they are the hardest to separate. In the second problem, we consider the separation between male people with or without mustaches on the CelebA dataset [18] (unbalanced classes, 11779 training (36% with mustache), 11036 test samples (37%)).

Table 1 compares the classification accuracy and the adversarial robustness results for the three types of classifiers. The drop in accuracy for the proposed solution, compared to classical networks, is less than one point even for a complex task such as celeb-A moustache classification. The last column of the table compares the average L_2 norm of adversarial noise for the three types of classifier. On the MNIST dataset, the improvement of robustness with 1-Lipschitz layers is significant with a clear advantage for our approach. When considering the CelebA problem, using 1-Lipschitz layers with log-entropy is not enough (the *logit* values tend to be small). The proposed hKR approach leads to a classifier that is up to 10 times more robust than its competitors with an acceptable loss of accuracy.

In Fig. 3, we compare, on the MNIST 0-8 dataset, the L_2 norm of adversarial samples with respect to the output of the hKR neural networks (and the logit values for the 1LIP network). Figures 3a and 3b show that with our proposed learning rule, the fooling noise for a given input is linearly linked to the output (slope of one for MLP, and around 1.1 for CNN), which confirms that the Lipschitz constants of our networks are very close to (but lower than) 1. We also observe that, for a given input sample, the network prediction represents a very tight lower bound of the adversarial robustness of the network for this sample. In contrast, for the 1LIP-MLP (Fig. 3c), the 1-Lipschitz constraint is also guaranteed, but the output of the network can be far lower than the adversarial noise norm. While on some samples at the tail end of the distribution, the L_2 norm of found noise can reach 30, the average adversarial robustness is lower than for the proposed solution (green vertical lines). Beside the level of noise, Figures 4 empirically show that, in contrast to the other approaches, the noise required to change the output class for the hKR classifier is highly structured, and interpretable. Thus, on the MNIST 0-8 dataset, in order to fool the proposed learned network with *DeepFool*, a 0-image, for instance, is explicitly transformed into a mix between an 8 and a 0. Even for a more complex task, such as a mustache classifier on the CelebA dataset, Fig. 5 shows that fooling an image of a male without (resp. with) a mustache requires to addition (resp. removal) of dark pixels around the nasolabial fold. We also build counterfactual examples (line d) by applying the scheme proposed in Section 3.2 (i.e. $\text{counter}(\hat{f}, \mathbf{x}) \approx \mathbf{x} - c_x * \hat{f}(\mathbf{x}) * \nabla_{\mathbf{x}} \hat{f}(\mathbf{x})$). For each sample, we choose c_x to obtain a visually satisfactory counterfactual (and not at the classification boundary as for adversarial examples). Although the differential images are not as precise as the ones obtained with adversarial approach, they clearly focus on the meaningful part of the images and provide, in our opinion, convincing counterfactual explanations. Remark that this approach is closely related to saliency map. However, the results obtained with our network are far more precise than the ones on classical networks.

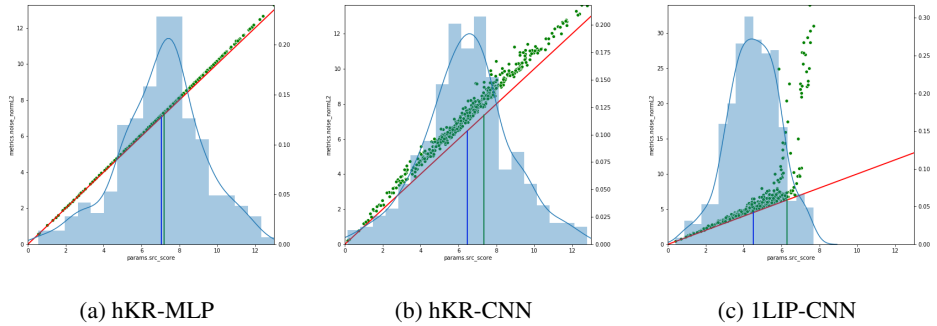


Figure 3: Comparison of L_2 norm of fooling noise (Y-axis) with the *output* value (X-axis): green dots noise norm for samples (green line average value), red line: minimal possible noise (1-lipschitz), blue histogram: *output* (resp. *logit* for 1LIP-CNN) distribution (blue line average value)

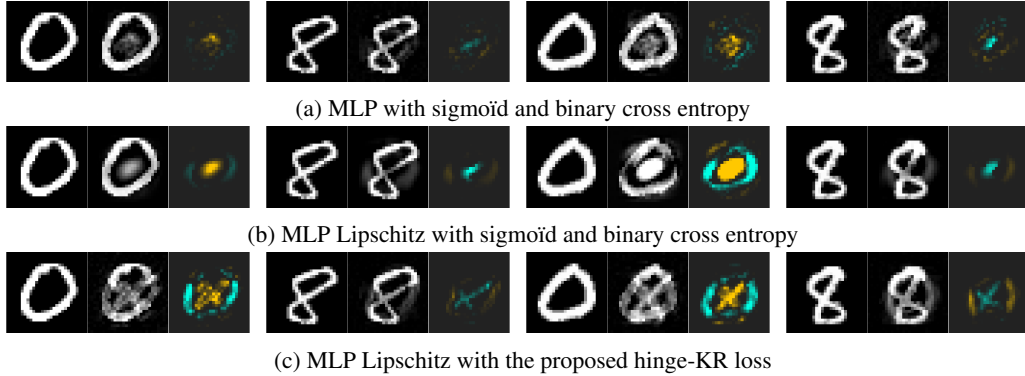


Figure 4: Deepfool adversarial examples on MNIST 0-8 dataset: source image, fooled image, differential image (yellow (resp. cyan) increase (resp. decrease) grey level)

6 Conclusion and future works

This paper presents a novel binary classification framework and the associated deep learning process. Besides the interpretation of the classification task as a regularized optimal transport problem, we demonstrate that this new formalization has some valuable properties about error bounds and robustness regarding adversarial attacks. We also propose a systematic approach to ensure the 1-Lipschitz constraint of a neural network. This includes a state-of-the-art regularization algorithm and more precise constant evaluation for convolutional and pooling layers. Even if this regularization process can increase the computation time during learning, it doesn't impact inference. We developed an open source python library based on tensorflow for 1-Lipshitz layers and gradient preserving activation and pooling functions. This makes the approach very easy to implement and to use.

The experiment emphasizes the theoretical results and confirms that the classifier has good and predictable robustness to adversarial attack with a acceptable cost on accuracy. We also show that our classifier forces adversarial attacks to explicitly modify the input. Moreover, we show that we can easily build counterfactuals explanations. This suggest that with our novel classification problem, the adversarial attack is linked to the optimal transportation.

In conclusion, we believe that this classification framework based on optimal transport is of great interest for critical problems since it provides both empirical and theoretical guarantees. Future works will focus on the multiclass counterpart of the approach and on its applicability to large and deep networks.

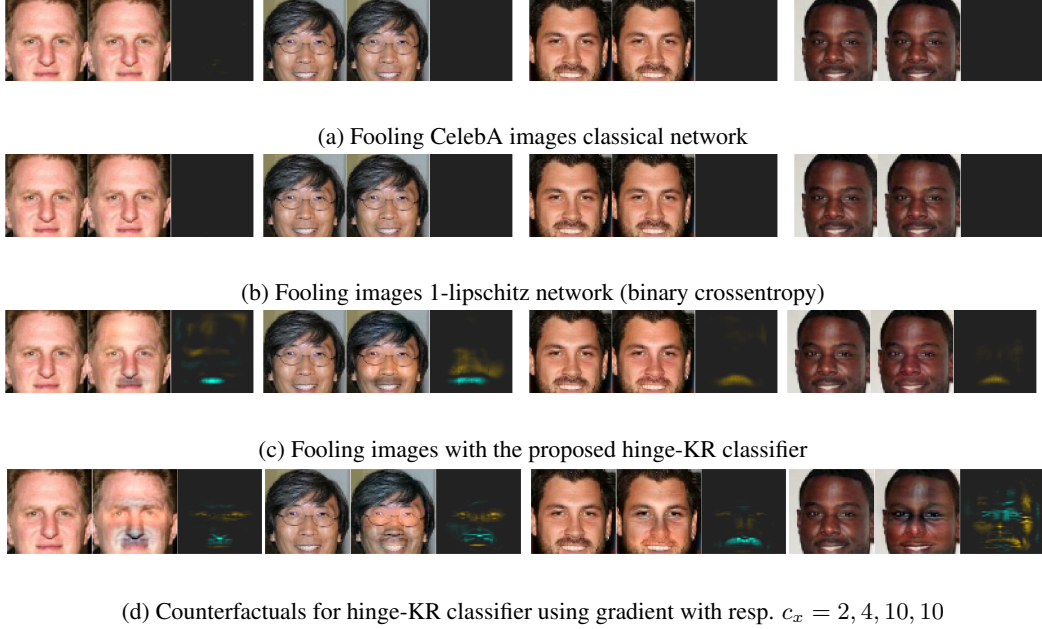


Figure 5: (a-c) Deepfool and adversarial examples on Celeb-A dataset: two left (resp. right) triplet-images without (resp. with) mustache. Triplet-images consist of source image, fooled image, and differential image of V channel in HSV colorspace (yellow (resp. cyan) increase (resp. decrease) V channel level) with a common color scale for all settings. (d) counterfactuals: the last images of the triplets are $\nabla_x \hat{f}(\mathbf{x})$ with the same color representation than differential images.

Acknowledgments and Disclosure of Funding

This project received funding from the French Investing for the Future PIA3 program within the Artificial and Natural Intelligence Toulouse Institute (ANITI). The authors gratefully acknowledge the support of the DEEL project².

References

- [1] Cem Anil, James Lucas, and Roger Grosse. Sorting out Lipschitz function approximation. In Kamalika Chaudhuri and Ruslan Salakhutdinov, editors, *Proceedings of the 36th International Conference on Machine Learning*, volume 97 of *Proceedings of Machine Learning Research*, pages 291–301, Long Beach, California, USA, 09–15 Jun 2019. PMLR.
- [2] Martin Arjovsky, Soumith Chintala, and Léon Bottou. Wasserstein generative adversarial networks. In Doina Precup and Yee Whye Teh, editors, *Proceedings of the 34th International Conference on Machine Learning*, volume 70 of *Proceedings of Machine Learning Research*, pages 214–223, International Convention Centre, Sydney, Australia, 06–11 Aug 2017. PMLR.
- [3] Åke Björck and C. Bowie. An Iterative Algorithm for Computing the Best Estimate of an Orthogonal Matrix. *SIAM Journal on Numerical Analysis*, 8(2):358–364, June 1971.
- [4] Y. Lan Boureau, Jean Ponce, and Yann Lecun. A theoretical analysis of feature pooling in visual recognition. In *ICML 2010 - Proceedings, 27th International Conference on Machine Learning*, ICML 2010 - Proceedings, 27th International Conference on Machine Learning, pages 111–118, September 2010. 27th International Conference on Machine Learning, ICML 2010 ; Conference date: 21-06-2010 Through 25-06-2010.
- [5] Haim Brezis. *Function Analysis, Sobolev Spaces and Partial Differential Equations*. Springer, 01 2010.

²<https://www.deel.ai/>

[6] Moustapha Cisse, Piotr Bojanowski, Edouard Grave, Yann Dauphin, and Nicolas Usunier. Parseval Networks: Improving Robustness to Adversarial Examples. *arXiv:1704.08847 [cs, stat]*, April 2017. arXiv: 1704.08847.

[7] Mélanie Ducoffe, Sébastien Gerchinovitz, and Jayant Sen Gupta. A high-probability safety guarantee for shifted neural network surrogates. In *SafeAI*, 02 2020.

[8] Martín Abadi et al. TensorFlow: Large-scale machine learning on heterogeneous systems, 2015. Software available from tensorflow.org.

[9] Rémi Flamary and Nicolas Courty. Pot python optimal transport library, 2017.

[10] Wilfrid Gangbo and Robert McCann. The geometry of optimal transportation. *Acta Mathematica*, 177:113–161, 09 1996.

[11] Gene H. Golub and Henk A. van der Vorst. Eigenvalue computation in the 20th century. *Journal of Computational and Applied Mathematics*, 123(1):35 – 65, 2000. Numerical Analysis 2000. Vol. III: Linear Algebra.

[12] Ian Goodfellow, Jean Pouget-Abadie, Mehdi Mirza, Bing Xu, David Warde-Farley, Sherjil Ozair, Aaron Courville, and Yoshua Bengio. Generative adversarial nets. In Z. Ghahramani, M. Welling, C. Cortes, N. D. Lawrence, and K. Q. Weinberger, editors, *Advances in Neural Information Processing Systems 27*, pages 2672–2680. Curran Associates, Inc., 2014.

[13] Ishaan Gulrajani, Faruk Ahmed, Martín Arjovsky, Vincent Dumoulin, and Aaron C. Courville. Improved training of wasserstein gans. *CoRR*, abs/1704.00028, 2017.

[14] Kaiming He, Xiangyu Zhang, Shaoqing Ren, and Jian Sun. Deep Residual Learning for Image Recognition. *arXiv:1512.03385 [cs]*, December 2015. arXiv: 1512.03385.

[15] Kaiming He, Xiangyu Zhang, Shaoqing Ren, and Jian Sun. Delving deep into rectifiers: Surpassing human-level performance on imagenet classification. *2015 IEEE International Conference on Computer Vision (ICCV)*, Dec 2015.

[16] Matthias Hein and Maksym Andriushchenko. Formal Guarantees on the Robustness of a Classifier against Adversarial Manipulation. *arXiv:1705.08475 [cs, stat]*, May 2017.

[17] Yann Lecun, Léon Bottou, Yoshua Bengio, and Patrick Haffner. Gradient-based learning applied to document recognition. In *Proceedings of the IEEE*, pages 2278–2324, 1998.

[18] Ziwei Liu, Ping Luo, Xiaogang Wang, and Xiaoou Tang. Deep learning face attributes in the wild. In *Proceedings of International Conference on Computer Vision (ICCV)*, December 2015.

[19] Takeru Miyato, Toshiki Kataoka, Masanori Koyama, and Yuichi Yoshida. Spectral normalization for generative adversarial networks. *ArXiv*, abs/1802.05957, 2018.

[20] Seyed-Mohsen Moosavi-Dezfooli, Alhussein Fawzi, and Pascal Frossard. DeepFool: a simple and accurate method to fool deep neural networks. *arXiv:1511.04599 [cs]*, November 2015. arXiv: 1511.04599.

[21] Hajime Ono, Tsubasa Takahashi, and Kazuya Kakizaki. Lightweight Lipschitz Margin Training for Certified Defense against Adversarial Examples. *arXiv:1811.08080 [cs, stat]*, November 2018. arXiv: 1811.08080.

[22] Haifeng Qian and Mark N. Wegman. L2-nonexpansive neural networks. In *International Conference on Learning Representations*, 2019.

[23] Jonas Rauber, Wieland Brendel, and Matthias Bethge. Foolbox: A Python toolbox to benchmark the robustness of machine learning models. *arXiv:1707.04131 [cs, stat]*, March 2018. arXiv: 1707.04131.

[24] R . Tyrrell Rockafellar and Roger Wets. *Variational Analysis*, volume 317. Springer, 01 2004.

- [25] Tim Salimans and Diederik P. Kingma. Weight normalization: A simple reparameterization to accelerate training of deep neural networks. *CoRR*, abs/1602.07868, 2016.
- [26] Jure Sokolic, Raja Giryes, Guillermo Sapiro, and Miguel R. D. Rodrigues. Robust large margin deep neural networks. *IEEE Transactions on Signal Processing*, 65(16):42654280, Aug 2017.
- [27] Christian Szegedy, Wojciech Zaremba, Ilya Sutskever, Joan Bruna, Dumitru Erhan, Ian Goodfellow, and Rob Fergus. Intriguing properties of neural networks, 2013.
- [28] Christian Szegedy, Wojciech Zaremba, Ilya Sutskever, Joan Bruna, Dumitru Erhan, Ian Goodfellow, and Rob Fergus. Intriguing properties of neural networks. *arXiv:1312.6199 [cs]*, December 2013.
- [29] Dimitris Tsipras, Shibani Santurkar, Logan Engstrom, Alexander Turner, and Aleksander Madry. Robustness may be at odds with accuracy, 2018.
- [30] Cédric Villani. *Optimal Transport: Old and New.* Grundlehren der mathematischen Wissenschaften. Springer Berlin Heidelberg, 2008.
- [31] Aladin Virmaux and Kevin Scaman. Lipschitz regularity of deep neural networks: analysis and efficient estimation. In S. Bengio, H. Wallach, H. Larochelle, K. Grauman, N. Cesa-Bianchi, and R. Garnett, editors, *Advances in Neural Information Processing Systems 31*, pages 3835–3844. Curran Associates, Inc., 2018.
- [32] Sandra Wachter, Brent D. Mittelstadt, and Chris Russell. Counterfactual explanations without opening the black box: Automated decisions and the GDPR. *CoRR*, abs/1711.00399, 2017.

A Optimal transportation : discrete case

A.1 Optimal transport

When considering a limited number of samples for the two distribution, the computation of the Wasserstein distance can be solved through linear programming algorithms. In the balanced case, we have $X = \{x_1, \dots, x_{2n}\}$ where $\{x_1, \dots, x_n\}$ are sampled from P_+ and $\{x_{n+1}, \dots, x_{2n}\}$ are sampled from P_- . We note $U = \{u_1, \dots, u_{2n}\}$ the labels with $u_1, \dots, u_n = 1$ and $u_{n+1}, \dots, u_{2n} = -1$ and C the $n \times n$ matrix cost function with $C_{i,j} = \|x_i - x_{n+j}\|$. The primal problem of the optimal transport is to find a transportation plan Π (a $n \times n$ matrix) such as:

$$\min_{\Pi} \quad \sum_{i,j \in n \times n} \Pi_{i,j} * C_{i,j} \quad (14)$$

$$\text{subject to} \quad \Pi_{i,j} \geq 0, \quad (15)$$

$$\sum_i \Pi_{i,j} = \frac{1}{n}, \sum_j \Pi_{i,j} = \frac{1}{n}. \quad (16)$$

The constraints enforce Π to be a discrete joint probability distribution with the appropriate marginals as in the continuous case. The dual formulation for the discrete optimal transport problem is:

$$\max_F \quad F \cdot U^T \quad (17)$$

$$\text{subject to} \quad \forall i, j \in n \times n, F_i - F_{n+j} \leq C_{i,j} \quad (18)$$

where F is a $2n$ vector that is a discrete version of the function f of Equation 1b. The constraint on F is the discrete counterpart of the 1-Lipschitz constraint.

A.2 Hinge regularized Optimal transport

Similarly to the classical case, the discrete counterpart of the regularized Wasserstein distance is also a transportation problem which has the following formulation:

$$\begin{aligned} \min_{\Pi} \quad & \sum_{i,j \in n \times n} [\Pi_{i,j} * C_{i,j}] - 2 \left(1 - \sum_{i,j \in n \times n} [\Pi_{i,j}] \right) \\ \text{subject to} \quad & \Pi_{i,j} \geq 0, \\ & \frac{1}{n} \leq \sum_i \Pi_{i,j} \leq \frac{1+\lambda}{n}, \\ & \frac{1}{n} \leq \sum_j \Pi_{i,j} \leq \frac{1+\lambda}{n}. \end{aligned}$$

Roughly speaking, it allows to give more weight to the transportation of the closest pairs by admitting to deviate from the marginals with a tolerance that depends on λ . Since the closest pairs in the two distributions are the most difficult to classify, it illustrates why this formulation is more adequate for classification problem. The dual formulation of this transportation problem is a discrete counterpart of Equation 5 :

$$\begin{aligned} \max_F \quad & \sum_{k=0}^{2n} [F_k * u_k - \lambda(0, 1 - F_k * u_k)_+] \\ \text{subject to} \quad & \forall i, j \in n \times n, F_i - F_{n+j} \leq C_{i,j}. \end{aligned}$$

We observe that the constraint in the dual problem are not affected by the new formulation and still corresponds to a the 1-Lipschitz constraint in the continuous case.

B Theorem proofs

B.1 Proof Theorem 1

We denote as

$$f^* := f_\lambda^* \in \arg \min_{f \in \text{Lip}_1(\Omega)} \mathcal{L}_\lambda^{hKR}(f) \quad \text{and} \quad \hat{f}_n := \hat{f}_{n,\lambda} \in \arg \min_{f \in \text{Lip}_1(\Omega)} \hat{\mathcal{L}}_{\lambda,n}^{hKR}(f). \quad (19)$$

If we assume that (6) is not true, then there exists $\mathbf{x} \in \Omega$ such that $f^*(\mathbf{x}) > 1 + \text{diam}(\Omega) + \frac{\mathcal{R}(\psi)}{\inf(p, 1-p)}$ or $f^*(\mathbf{x}) < -1 - \text{diam}(\Omega) - \frac{L_1(\psi)}{\inf(p, 1-p)}$. We suppose without loss of generality that the first inequality holds. If $\mathbf{z} \in \Omega$ then the 1-Lipschitz condition in f^* implies that $f^*(\mathbf{z}) > 1 + \frac{L_1(\psi)}{1-p}$. Hence $(1 - f^*)_+ = 0$ and

$$\begin{aligned} L(f^*) &\leq \sup_{g \in \text{Lip}_1(\Omega)} L_2(g) - \lambda L_1(f^*) \\ &= \sup_{g \in \text{Lip}_1(\Omega)} E_{X|Y=1}(g(X)) - E_{X|Y=-1}(g(X)) - E\{\lambda(1 - Yf^*(X))_+\} \\ &= L_2(\psi) - \lambda\{pE_{X|Y=1}(1 - f^*(X))_+ + (1-p)E_{X|Y=-1}(1 + f^*(X))_+\} \\ &\leq L_2(\psi) - \lambda\{(1-p)E_{X|Y=-1}(1 + f^*(X))\} \\ &\leq L_2(\psi) - \lambda\{(1-p)E_{X|Y=-1}(2 + \frac{L_1(\psi)}{1-p})\} \\ &= L_2(\psi) - 2\lambda(1-p) - \lambda\{E_{X|Y=-1}(L_1(\psi))\} = L_2(\psi) - 2\lambda(1-p) - \lambda L_1(\psi) \end{aligned}$$

Then f^* can not be an optimal solution of the problem (19). Then there exists some constant M large enough, such that f^* belongs to $\text{Lip}_1^M(\Omega) := \{f \in \text{Lip}_1(\Omega) : \|f\|_\infty \leq M\}$ and not to $\text{Lip}_1(\Omega)$. Since the functional $\mathcal{L}_\lambda^{hKR}$ is convex and $\text{Lip}_1^M(\Omega)$ is compact in $\mathcal{C}(\Omega)$, we are able to make use of Ascoli-Arzela Theorem and conclude that there exists at least one function minimizing the expected loss. Furthermore the set of those functions is compact and convex.

B.2 Proof Theorem 2

Definition B.1. Let μ, ν two positive measures in \mathbb{R}^d . The Kullback-Leibler divergence from μ to ν is defined as

$$KL(\mu|\nu) = \begin{cases} \int \log(\frac{d\mu}{d\nu}) d\mu - \int d\mu + \int d\nu & \text{if } \mu \ll \nu \\ \infty & \text{otherwise} \end{cases} \quad (20)$$

Theorem 3. Let $\phi_1, \phi_2 : \Omega \rightarrow \bar{\mathbb{R}}$ be lower semicontinuous convex functions and $\mu, \nu \in \mathcal{P}(\Omega)$ be probability measures. Then for all $\epsilon > 0$ the following equality holds

$$\begin{aligned} &\inf_{\pi \in \Pi_+(\mu, \nu)} \int \phi_1(-\frac{d\pi_{\mathbf{x}}}{d\mu}(\mathbf{x})) d\mu(\mathbf{x}) + \int \phi_2(-\frac{d\pi_{\mathbf{z}}}{d\nu}(\mathbf{z})) d\nu(\mathbf{z}) + \epsilon KL(\pi | e^{-\frac{c(\mathbf{x}, \mathbf{z})}{\epsilon}} (d\mu \times d\nu)) \\ &= \sup_{f, g \in L^1(\Omega)} - \int_{\Omega} \phi_1^*(f(\mathbf{x})) d\mu(\mathbf{x}) - \int_{\Omega} \phi_2^*(g(\mathbf{z})) d\nu(\mathbf{z}) - \epsilon \int \left(e^{\frac{f(\mathbf{x}) + g(\mathbf{z}) - c(\mathbf{x}, \mathbf{z})}{\epsilon}} - e^{-\frac{c(\mathbf{x}, \mathbf{z})}{\epsilon}} \right) d\mu d\nu. \end{aligned} \quad (21)$$

Furthermore if $\epsilon = 0$ then

$$\begin{aligned} &\inf_{\pi \in \Pi_+(\mu, \nu)} \int_{\Omega \times \Omega} c(\mathbf{x}, \mathbf{z}) d\pi(\mathbf{x}, \mathbf{z}) + \int \phi_1(-\frac{d\pi_{\mathbf{x}}}{d\mu}(\mathbf{x})) d\mu(\mathbf{x}) + \int \phi_2(-\frac{d\pi_{\mathbf{z}}}{d\nu}(\mathbf{z})) d\nu(\mathbf{z}) \\ &= \sup_{(f, g) \in \Phi(\mu, \nu)} - \int_{\Omega} \phi_1^*(f(\mathbf{x})) d\mu(\mathbf{x}) - \int_{\Omega} \phi_2^*(g(\mathbf{z})) d\nu(\mathbf{z}). \end{aligned} \quad (22)$$

Where $\Pi_+(\mu, \nu)$ is the set of positive measures $\pi \in \mathcal{M}_+(\Omega \times \Omega)$ which are absolutely continuous with respect to the joint measure $d\mu \times d\nu$, and $\Phi(\mu, \nu)$ consists of the pairs of functions $(f, g) \in L_1(\Omega) \times L_1(\Omega)$ such that $c(\mathbf{x}, \mathbf{z}) - f(\mathbf{x}) - g(\mathbf{z}) \geq 0$ $d\mu \times d\nu$ a.s..

First we recall the FenchelRockafellar Duality result, we use a weaker version given in Theorem 1.12 in [5]

Proposition 3. Let E be a Banach space and $\Upsilon, \Psi : E \rightarrow \mathbb{R} \cup \{\infty\}$ be two convex functions, assume that there exist $z_0 \in \text{dom}(\Psi) \cap \text{dom}(\Upsilon)$ such that Ψ is continuous in z_0 . Then strong duality holds

$$\inf_{a \in E} \{\Upsilon(a) + \Psi(a)\} = \sup_{b \in E^*} \{-\Upsilon^*(-b) - \Psi^*(b)\} \quad (23)$$

We identify the different elements of our problem with such of previous Proposition.

- E is the space of continuous functions in $\Omega \times \Omega$. Note that the set is bounded, hence E^* , by Riesz theorem, is the set of regular measures in $\Omega \times \Omega$.
- If $\epsilon = 0$:

$$\Psi_0(u) = \begin{cases} 0 & \text{if } u(\mathbf{x}, \mathbf{z}) \geq -c(\mathbf{x}, \mathbf{z}) \\ \infty & \text{otherwise} \end{cases} \quad (24)$$

$$\Upsilon_0(u) = \begin{cases} \int \phi_1^*(-f(\mathbf{x})) d\mu(\mathbf{x}) + \int \phi_2^*(-g(\mathbf{z})) d\nu(\mathbf{z}) & \text{if } u(\mathbf{x}, \mathbf{z}) = f(\mathbf{x}) + g(\mathbf{z}) \\ \infty & \text{otherwise} \end{cases} \quad (25)$$

If $\epsilon > 0$:

$$\Psi_\epsilon(u) = \epsilon \int \left(e^{\frac{u(\mathbf{x}, \mathbf{z}) - c(\mathbf{x}, \mathbf{z})}{\epsilon}} - e^{-\frac{c(\mathbf{x}, \mathbf{z})}{\epsilon}} \right) d\mu(\mathbf{x}) d\nu(\mathbf{z}) \quad (26)$$

$$\Upsilon_\epsilon(u) = \Upsilon_0(u) \quad (27)$$

Note that $\Upsilon_\epsilon(u) = \Upsilon_0(u)$ could be non well defined, to avoid this situation we fix $\mathbf{x}_0 \in \Omega$ and consider $u(\mathbf{x}, \mathbf{z}) = (u(\mathbf{x}, \mathbf{z}_0) - u(\mathbf{z}_0, \mathbf{z}_0)/2) + u(\mathbf{z}_0, \mathbf{z}) - u(\mathbf{z}_0, \mathbf{z}_0)/2$. Now we compute the dual operators

$$\begin{aligned} \Psi_\epsilon^*(-\pi) &= \sup_{u \in E} \left\{ -\epsilon \int \left(e^{\frac{u(\mathbf{x}, \mathbf{z}) - c(\mathbf{x}, \mathbf{z})}{\epsilon}} - e^{-\frac{c(\mathbf{x}, \mathbf{z})}{\epsilon}} \right) d\mu(\mathbf{x}) d\nu(\mathbf{z}) - \int u(\mathbf{x}, \mathbf{z}) d\pi(\mathbf{x}, \mathbf{z}) \right\} \\ &= \sup_{u \in E} \left\{ -\epsilon \int \left(e^{\frac{u(\mathbf{x}, \mathbf{z}) - c(\mathbf{x}, \mathbf{z})}{\epsilon}} - e^{-\frac{c(\mathbf{x}, \mathbf{z})}{\epsilon}} \right) d\mu(\mathbf{x}) d\nu(\mathbf{z}) + \int u(\mathbf{x}, \mathbf{z}) d\pi(\mathbf{x}, \mathbf{z}) \right\} \end{aligned}$$

Now if π were not absolutely continuous respect the joint measure $e^{-\frac{c(\mathbf{x}, \mathbf{z})}{\epsilon}} d\mu \times d\nu$ then we would have a continuous function $u(\mathbf{x}, \mathbf{z}) = 0 d\mu \times d\nu$ almost surely and such that $\int u(\mathbf{x}, \mathbf{z}) d\pi(\mathbf{x}, \mathbf{z}) \neq 0$. If we take the function $\lambda u(\mathbf{z}, \mathbf{z})$ and λ tends to $\pm\infty$ we deduce that the supremum is ∞ . Then suppose that $d\pi = m(\mathbf{x}, \mathbf{z}) e^{-\frac{c(\mathbf{x}, \mathbf{z})}{\epsilon}} (d\mu \times d\nu)$.

$$\begin{aligned} \Psi_\epsilon^*(-\pi) &= \begin{cases} \sup_{u \in E} \left\{ \epsilon \int \left(-e^{\frac{u(\mathbf{x}, \mathbf{z})}{\epsilon}} + 1 + \frac{u(\mathbf{x}, \mathbf{z})}{\epsilon} m(\mathbf{x}, \mathbf{z}) \right) e^{-\frac{c(\mathbf{x}, \mathbf{z})}{\epsilon}} d\mu(\mathbf{x}) d\nu(\mathbf{z}) \right\} & \text{if } d\pi = m e^{-\frac{c(\mathbf{x}, \mathbf{z})}{\epsilon}} (d\mu \times d\nu) \\ \infty & \text{otherwise.} \end{cases} \\ &= \epsilon K L(\pi | e^{-\frac{c(\mathbf{x}, \mathbf{z})}{\epsilon}} (d\mu \times d\nu)) \end{aligned}$$

With some similar calculation, we compute for $\epsilon = 0$:

$$\Psi_0^*(-\pi) = \begin{cases} \int c(\mathbf{x}, \mathbf{z}) d\pi(\mathbf{x}, \mathbf{z}) & \text{if } \pi \text{ is a positive measure.} \\ \infty & \text{otherwise.} \end{cases}$$

Finally for $\Upsilon_\epsilon^* = \Upsilon_0^*$

$$\begin{aligned} \Upsilon_\epsilon^*(\pi) &= \sup_{u \in E, u(\mathbf{x}, \mathbf{z}) = f(\mathbf{x}) + g(\mathbf{z})} \left\{ \int f(\mathbf{x}) + g(\mathbf{z}) d\pi(\mathbf{x}, \mathbf{z}) - \int \phi_1^*(-f(\mathbf{x})) d\mu(\mathbf{x}) - \int \phi_2^*(-g(\mathbf{z})) d\nu(\mathbf{z}) \right\} \\ &= \sup_{u \in E, u(\mathbf{x}, \mathbf{z}) = f(\mathbf{x}) + g(\mathbf{z})} \left\{ \int f(\mathbf{x}) d\pi_{\mathbf{x}}(\mathbf{x}) - \int \phi_1^*(-f(\mathbf{x})) d\mu(\mathbf{x}) + \int g(\mathbf{z}) d\pi_{\mathbf{z}}(\mathbf{z}) - \int \phi_2^*(-g(\mathbf{z})) d\nu(\mathbf{z}) \right\} \\ &= \sup_{f \in C(\Omega)} \left\{ \int f(\mathbf{x}) d\pi_{\mathbf{x}}(\mathbf{x}) - \int \phi_1^*(-f(\mathbf{x})) d\mu(\mathbf{x}) \right\} + \sup_{g \in C(\Omega)} \left\{ \int g(\mathbf{z}) d\pi_{\mathbf{z}}(\mathbf{z}) - \int \phi_2^*(-g(\mathbf{z})) d\nu(\mathbf{z}) \right\} \\ &= (I_1) + (I_2). \end{aligned}$$

We first consider (I_1) . The same reasoning will hold for (I_2) . If $\pi_{\mathbf{x}}$ were not absolutely continuous respect μ then reasoning as before we obtain ∞ . Then $d\pi_{\mathbf{x}} = \frac{d\pi_{\mathbf{x}}}{d\mu} d\mu$ and

$$\begin{aligned} (I_1) &= \sup_{f \in C(\Omega)} \left\{ \int \left(-f(\mathbf{x}) \frac{d\pi_{\mathbf{x}}}{d\mu} - \phi_1^*(f(\mathbf{x})) \right) d\mu(\mathbf{x}) \right\} \\ &= \int \left(\sup_m \left\{ -\frac{d\pi_{\mathbf{x}}}{d\mu} m - \phi_1^*(m) \right\} \right) d\mu(\mathbf{x}) = \int \phi_1(-\frac{d\pi_{\mathbf{x}}}{d\mu}) d\mu(\mathbf{x}) \\ (I_2) &= \int \phi_2(-\frac{d\pi_{\mathbf{x}}}{d\nu}) d\mu(\mathbf{z}) \end{aligned}$$

Note that the inversion of the supremum and the integral is guaranteed here since $(\mathbf{x}, m) \mapsto -m \frac{d\pi_{\mathbf{x}}}{d\mu}(\mathbf{x}) + \phi_1^*(m)$ is lower semi-continuous and convex in m and measurable in (\mathbf{x}, m) . Then it is a normal integrand, and we can apply Theorem 14.60 in [24].

Then computing both in Equation (23) we end with the following result

$$\begin{aligned} &\inf_{u(\mathbf{x}, \mathbf{z}) = f(\mathbf{x}) + g(\mathbf{z}) \geq -c(\mathbf{x}, \mathbf{z})} \left\{ \int \phi_1^*(-f(\mathbf{x})) d\mu(\mathbf{x}) + \int \phi_2^*(-g(\mathbf{z})) d\nu(\mathbf{z}) \right\} \\ &= \inf_{f(\mathbf{x}) + g(\mathbf{z}) \leq c(\mathbf{x}, \mathbf{z})} \left\{ \int \phi_1^*(f(\mathbf{x})) d\mu(\mathbf{x}) + \int \phi_2^*(g(\mathbf{z})) d\nu(\mathbf{z}) \right\} \\ &= - \sup_{f(\mathbf{x}) + g(\mathbf{z}) \leq c(\mathbf{x}, \mathbf{z})} \left\{ - \int \phi_1^*(f(\mathbf{x})) d\mu(\mathbf{x}) - \int \phi_2^*(g(\mathbf{z})) d\nu(\mathbf{z}) \right\} \\ &\sup_{\pi \in \mathcal{M}_+(\Omega \times \Omega)} \left\{ - \int c(\mathbf{x}, \mathbf{z}) d\pi(\mathbf{x}, \mathbf{z}) - \int \phi_2(-\frac{d\pi_{\mathbf{x}}}{d\nu}) d\mu(\mathbf{z}) - \int \phi_1(-\frac{d\pi_{\mathbf{x}}}{d\mu}) d\mu(\mathbf{x}) \right\} \\ &= - \inf_{\pi \in \mathcal{M}_+(\Omega \times \Omega)} \left\{ \epsilon \int c(\mathbf{x}, \mathbf{z}) d\pi(\mathbf{x}, \mathbf{z}) + \int \phi_2(-\frac{d\pi_{\mathbf{x}}}{d\nu}) d\mu(\mathbf{z}) + \int \phi_1(-\frac{d\pi_{\mathbf{x}}}{d\mu}) d\mu(\mathbf{x}) \right\}. \\ &\inf_{u(\mathbf{x}, \mathbf{z}) = f(\mathbf{x}) + g(\mathbf{z})} \left\{ \epsilon \int \left(e^{\frac{-f(\mathbf{x}) - g(\mathbf{z}) - c(\mathbf{x}, \mathbf{z})}{\epsilon}} - e^{-\frac{c(\mathbf{x}, \mathbf{z})}{\epsilon}} \right) d\mu(\mathbf{x}) d\nu(\mathbf{z}) + \int \phi_1^*(-f(\mathbf{x})) d\mu(\mathbf{x}) + \int \phi_2^*(-g(\mathbf{z})) d\nu(\mathbf{z}) \right\} \\ &= \inf_{f, g} \left\{ \epsilon \int \left(e^{\frac{f(\mathbf{x}) + g(\mathbf{z}) - c(\mathbf{x}, \mathbf{z})}{\epsilon}} - e^{-\frac{c(\mathbf{x}, \mathbf{z})}{\epsilon}} \right) d\mu(\mathbf{x}) d\nu(\mathbf{z}) + \int \phi_1^*(f(\mathbf{x})) d\mu(\mathbf{x}) + \int \phi_2^*(g(\mathbf{z})) d\nu(\mathbf{z}) \right\} \\ &= - \sup_{f, g} \left\{ -\epsilon \int \left(e^{\frac{f(\mathbf{x}) + g(\mathbf{z}) - c(\mathbf{x}, \mathbf{z})}{\epsilon}} - e^{-\frac{c(\mathbf{x}, \mathbf{z})}{\epsilon}} \right) d\mu(\mathbf{x}) d\nu(\mathbf{z}) - \int \phi_1^*(f(\mathbf{x})) d\mu(\mathbf{x}) - \int \phi_2^*(g(\mathbf{z})) d\nu(\mathbf{z}) \right\} \\ &\sup_{\pi \in \mathcal{M}_+(\Omega \times \Omega)} \left\{ -\epsilon KL(\pi | e^{-\frac{c(\mathbf{x}, \mathbf{z})}{\epsilon}} (d\mu \times d\nu)) - \int \phi_2(-\frac{d\pi_{\mathbf{x}}}{d\nu}) d\mu(\mathbf{z}) - \int \phi_1(-\frac{d\pi_{\mathbf{x}}}{d\mu}) d\mu(\mathbf{x}) \right\} \\ &= - \inf_{\pi \in \mathcal{M}_+(\Omega \times \Omega)} \left\{ \epsilon KL(\pi | e^{-\frac{c(\mathbf{x}, \mathbf{z})}{\epsilon}} (d\mu \times d\nu)) + \int \phi_2(-\frac{d\pi_{\mathbf{x}}}{d\nu}) d\mu(\mathbf{z}) + \int \phi_1(-\frac{d\pi_{\mathbf{x}}}{d\mu}) d\mu(\mathbf{x}) \right\} \end{aligned}$$

Proof of Theorem 2 With the same notation of Theorem 3, it is enough to consider, $\mu = P_+$ $\nu = P_-$ and

$$\psi_1(s) = \begin{cases} p - s & \text{if } s \in [p, p + \lambda p] \\ \infty & \text{else.} \end{cases} \quad (28)$$

$$\psi_2(s) = \begin{cases} 1 - p - s & \text{if } s \in [1 - p, 1 - p + \lambda(1 - p)] \\ \infty & \text{else.} \end{cases} \quad (29)$$

Then for each $f \in L_1(d\mu)$, $g \in L_1(d\nu)$

$$\begin{aligned} -\psi_1^*(f(\mathbf{x})) &= -\sup_s \{-\psi_1(s) + f(\mathbf{x})s\} = \inf_s \{\psi_1(-s) - f(\mathbf{x})s\} = \inf_s \{\psi_1(s) + f(\mathbf{x})s\} \\ &= \begin{cases} f(\mathbf{x}) & \text{if } 1 \leq f(\mathbf{x}) \\ f(\mathbf{x}) - p\lambda(1 - f(\mathbf{x})) & \text{else.} \end{cases} \\ &= f(\mathbf{x}) - p\lambda(1 - f(\mathbf{x}))_+ \\ -\psi_2^*(g(\mathbf{z})) &= f(\mathbf{z}) - (1 - p)\lambda(1 - f(\mathbf{z}))_+. \end{aligned}$$

Note that when $\lambda \geq 0$ the functions $r \mapsto h_1(r) := r - p\lambda(1 - r)_+$ and $h_2(r) := r - (1 - p)\lambda(1 - r)_+$ are nondecreasing. Now if we denote as J the right hand side of (21) then

$$J = \sup_{(f,g) \in \Phi(\mu,\nu)} \int_{\Omega} h_1(f(\mathbf{x}))d\mu(\mathbf{x}) + \int_{\Omega} h_2(g(\mathbf{z}))d\mu(\mathbf{z}).$$

We denote as f^d the d -conjugate of f defined as the function

$$f^d(r) := \inf_{s \in \Omega} \{|r - s| - f(s)\},$$

see for instance in [10] for a suitable definition. It is clear that $f^{dd} \geq f$, and the equality holds if f is a d -concave function since it is said that f is d -concave if it is the d -conjugate of another function. Hence using the nondecreasing condition of h we get to

$$J = \sup_{f^{dd}, f^d} \int_{\Omega} h_1(f^{dd}(\mathbf{x}))d\mu(\mathbf{x}) + \int_{\Omega} h_2(f^d(\mathbf{z}))d\mu(\mathbf{z}).$$

On the other side $f^d(r) = \inf_{s \in \Omega} \{|r - s| - f(s)\}$ is a limit of a sequence of 1-Lipschitz functions in Ω , hence it belongs to $\text{Lip}_1(\Omega)$. Using the 1-Lipschitz property and taking $r = s$ in the infimum leads to

$$-f^d(r) \leq \inf_{s \in \Omega} \{|r - s| - f^d(s)\} \leq -f^d(r).$$

This means that $f^{dd} = -f^d(r)$, hence we have that

$$\begin{aligned} J &= \sup_{(-f^d, f^d)} \int_{\Omega} h_1(f^{dd}(\mathbf{x}))d\mu(\mathbf{x}) + \int_{\Omega} h_2(f^d(\mathbf{z}))d\mu(\mathbf{z}) \\ &\leq \sup_{f \in \text{Lip}_1(\Omega)} \int_{\Omega} h_1(f^{dd}(\mathbf{x}))d\mu(\mathbf{x}) + \int_{\Omega} h_2(-f(\mathbf{z}))d\mu(\mathbf{z}) \leq J \end{aligned}$$

where the last inequality comes from the fact that if $f \in \text{Lip}_1(\Omega)$ then $(f, -f) \in \Phi(\mu, \nu)$.

B.3 Proof Proposition 1

As a direct consequence of Theorem 2 we derive the next equality

$$\begin{aligned} &\inf_{\pi \in \Pi_{\lambda}(P_+, P_-)} \int_{\Omega \times \Omega} \left(\frac{1}{\epsilon} |\mathbf{x} - \mathbf{z}| - 2 \right) d\pi + 2 \\ &= \sup_{f \in \text{Lip}_{1/\epsilon}(\Omega)} \int_{\Omega} f(dP_+ - dP_-) - \frac{\lambda}{2} \left(\int_{\Omega} (1 - f)_+ dP_+ + \int_{\Omega} (1 + f)_+ dP_- \right). \end{aligned} \tag{30}$$

We denote as I the left hand side of (30) and $\Pi(P_+, P_-)$ the set of measures with marginals P_+, P_- . Now using the hypothesis (10) we derive the next inequality

$$I = \inf_{\pi \in \Pi(P_+, P_-)} \int_{\Omega \times \Omega} \left(\frac{1}{\epsilon} |\mathbf{x} - \mathbf{z}| - 2 \right) d\pi + 2 = \frac{1}{\epsilon} \mathcal{W}(P_+, P_-).$$

Since $\text{Lip}_{1/\epsilon} \mathcal{W}(P_+, P_-) = \sup_{f \in \text{Lip}_{1/\epsilon}(\Omega)} \int_{\Omega} f(dP_+ - dP_-)$, we denote as $\psi_{\epsilon} \in \text{Lip}_{1/\epsilon}(\Omega)$ the function where the supremum is achieved. Hence we derive the following inequality

$$\begin{aligned} \frac{1}{\epsilon} \mathcal{W}(P_+, P_-) &= \int_{\Omega} f_{\lambda}(dP_+ - dP_-) - \lambda \left(\int_{\Omega} (1 - f_{\lambda})_+ dP_+ + \int_{\Omega} (1 + f_{\lambda})_+ dP_- \right) \\ &\leq \int_{\Omega} \psi_{\epsilon}(dP_+ - dP_-) - \lambda \left(\int_{\Omega} (1 - f_{\lambda})_+ dP_+ + \int_{\Omega} (1 + f_{\lambda})_+ dP_- \right) \\ &= \frac{1}{\epsilon} \mathcal{W}(P_+, P_-) - \lambda \left(\int_{\Omega} (1 - f_{\lambda})_+ dP_+ + \int_{\Omega} (1 + f_{\lambda})_+ dP_- \right). \end{aligned}$$

Then $\int_{\Omega} (1 - f_{\lambda})_+ dP_+ + \int_{\Omega} (1 + f_{\lambda})_+ dP_- = 0$ and the first assert of the proof is completed. The second assertion is a straightforward consequence of the previous one.

B.4 Proof Proposition 2

Even though the proof of Proposition 1 can be done following the frame of the proof of Proposition 1 in [13], we have provided here an easier proof in order to make this document self-content. The proof of this Proposition requires some properties on the transport plan.

Definition B.2. A set $\Gamma \subset \mathbb{R}^d \times \mathbb{R}^d$ is said to be *d-cyclically monotone* if for all $n \in \mathbb{N}$ and $\{(x_k, y_k)\}_{k=1}^n \subset \Gamma$ it is satisfied

$$\sum_{k=1}^n c(x_k, y_k) \leq \sum_{k=1}^n c(x_{k+1}, y_k), \text{ assuming that } n+1 = 1. \quad (31)$$

It is said that a measure is *d-cyclically monotone* if its support is *d-cyclically monotone*.

In particular the optimal transference plan in Kantorovich problem for the cost d is *d-cyclically monotone*, see Theorem 2.3 [10]. The same characterization holds for the optimal measures of (21), this claim is proved in the following Lemma.

Lemma 4. The optimal measure π of (21) is *d-cyclically monotone* for $d(\mathbf{x}, \mathbf{z}) = \|\mathbf{x} - \mathbf{z}\|$.

If π were not *d-cyclically monotone*, in [30] it is built another measure $\tilde{\pi}$, with the same marginals as π , such that the value of $\int |\mathbf{x} - \mathbf{z}| d\pi(\mathbf{x}, \mathbf{z}) > \int |\mathbf{x} - \mathbf{z}| \tilde{\pi}(\mathbf{x}, \mathbf{z})$. Computing this we deduce

$$\inf_{\pi \in \Pi_{\lambda}^p(\mu, \nu)} \int_{\Omega \times \Omega} |\mathbf{x} - \mathbf{z}| d\pi + \pi_{\mathbf{x}}(\Omega) + \pi_{\mathbf{z}}(\Omega) - 1 > \inf_{\tilde{\pi} \in \tilde{\Pi}_{\lambda}^p(\mu, \nu)} \int_{\Omega \times \Omega} |\mathbf{x} - \mathbf{z}| d\tilde{\pi} + \tilde{\pi}_{\mathbf{x}}(\Omega) + \tilde{\pi}_{\mathbf{z}}(\Omega) - 1.$$

Hence π cannot be optimal.

We replicate this construction on order to build this proof as self content as possible.

If P_+ and P_- are discrete probabilities. Then $P_+ = \sum_{k=1}^n u_k \delta_{\mathbf{x}_k}$ and $P_- = \sum_{j=1}^m v_j \delta_{\mathbf{z}_j}$ then the optimal measure has the form:

$$\frac{1}{n} \sum_{k,j=1}^n \pi_{k,j} \delta_{\mathbf{x}_k, \mathbf{z}_j} \quad (32)$$

If it is not *d-cyclically monotone* then there exist $N \in \mathbb{N}$ and $\{(\mathbf{x}_{k_i}, \mathbf{z}_{k_i})\}_{i=1}^N \subset \text{supp}(\pi)$ such that:

$$\sum_{i=1}^N \|\mathbf{x}_{k_i} - \mathbf{z}_{k_{i+1}}\| < \sum_{i=1}^N \|\mathbf{x}_{k_i} - \mathbf{z}_{k_i}\|, \text{ assuming that } k_{N+1} = k_1.$$

Let $a := \inf_{i=1, \dots, N} \{\pi_{k_i, k_i}\} > 0$. And let's define $\tilde{\pi}$ as

$$\tilde{\pi} := \pi + \frac{1}{n} \sum_{i=1}^n \left(\delta_{\mathbf{x}_{k_i}, \mathbf{z}_{k_{i+1}}} - \delta_{\mathbf{x}_{k_i}, \mathbf{z}_{k_i}} \right).$$

Then

$$\tilde{\pi}(A \times \Omega) = \pi(A \times \Omega) + \frac{1}{n} \sum_{i=1}^n \left(\delta_{\mathbf{x}_{k_i}}(A) - \delta_{\mathbf{x}_{k_i}}(A) \right) = \pi(A \times \Omega).$$

And the same holds with $(\Omega \times B)$ and the other marginal, and also it satisfied that

$$\frac{1}{n} \sum_{k,j=1}^n \|\mathbf{x}_k - \mathbf{z}_j\| \tilde{\pi}_{k,j} < \frac{1}{n} \sum_{k,j=1}^n \|\mathbf{x}_k - \mathbf{z}_j\| \pi_{k,j}.$$

Hence $\tilde{\pi}$ is the searched measure in the discrete case.

$\Pi_{\lambda}^p(\mathcal{S}, \mathcal{T})$ is sequentially compact respect the weak convergence denoted $*$ of measures if both \mathcal{S}, \mathcal{T} are also. Because of the compactness of $\Omega \times \Omega$, we only have to check that the set is bounded in total variation. But this is straightforward because for each $\pi \in \Pi_{\lambda}^p(P_+, P_-)$ it is satisfied $|\pi|(\Omega \times \Omega) \leq (p + p\lambda)(p + p\lambda)$.

If P_+ and P_- are general probabilities. Let X_1^+, \dots, X_n^+ and Z_1^+, \dots, Z_n^+ be sequences of independent random variables with law P_+ and P_- . And let P_n^+, P_n^- be the associated empirical measures. By using the strong law of large numbers we deduce that $P_n^+ \rightarrow P_+$ and $P_n^- \rightarrow P_-$ with probability one.

Now let π_n be the corresponding optimal measure for P_n^+, P_n^- , then there exist a measure π such that $\pi_n \rightharpoonup^* \pi$. It means that for each continuous and bounded function f in $\Omega \times \Omega$ we get

$$\int f d\pi_n \longrightarrow \int f d\pi.$$

Since the norm $(\mathbf{x}, \mathbf{z}) \mapsto \|\mathbf{x} - \mathbf{z}\|$ is continuous and bounded, once again because Ω is compact, we derive that

$$\int \|\mathbf{x} - \mathbf{z}\| d\pi_n + \pi_{\mathbf{x}_n}(\Omega) + \pi_{\mathbf{z}_n}(\Omega) - 1 \longrightarrow \int \|\mathbf{x} - \mathbf{z}\| d\pi + \pi_{\mathbf{x}}(\Omega) + \pi_{\mathbf{z}}(\Omega) - 1$$

Finally it is known that if a sequence of measures is d -cyclically monotone and converges weak* to another measure, then it is also d -cyclically monotone. This concludes the proof.

The proof of Proposition 1 is achieved as follows. The assumption of d -cyclically monotone involves that in particular $g(\mathbf{x}) - g(\mathbf{z}) = \|\mathbf{x} - \mathbf{z}\|$ π -a.s. for some function g . Then for the balanced case

$$\begin{aligned} & \int (g - 1) d\pi_x - \int (g + 1) d\pi_z + 2 \\ &= \sup_{f \in \text{Lip}_1(\Omega)} \int_{\Omega} f(dP_+ - dP_-) - \lambda \left(\int_{\Omega} (1 - f)_+ dP_+ + \int_{\Omega} (1 + f)_+ dP_- \right). \end{aligned}$$

Then we split $(g - 1) = (g - 1)\mathbf{1}_{g-1 \geq 0} + (g - 1)\mathbf{1}_{g-1 < 0}$ and

$$\begin{aligned} & \int (g - 1) d\pi_x + 1 \\ &= (1 + \lambda) \int (g - 1)\mathbf{1}_{g-1 \geq 0} dP_+ + \int (g - 1)\mathbf{1}_{g-1 < 0} dP_+ = \int (g - 1) - \lambda(1 - g)_+ dP_+. \end{aligned}$$

Doing the same with P_- , we deduce that this g is optimal and $g(\mathbf{x}) - g(\mathbf{z}) = \|\mathbf{x} - \mathbf{z}\|$ π -a.s. for the optimal measure π . As a consequence of such observations, following exactly the same arguments of the proof of Proposition 1 in [13], note that the key is $g(\mathbf{x}) - g(\mathbf{z}) = \|\mathbf{x} - \mathbf{z}\|$ π -a.s. which comes from what follows.

Let f^* be the optimal of Lemma 4, \mathbf{x} be a differentiable point of f^* . By assumption, the density property implies that $\pi(\mathbf{x} = \mathbf{z}) = 0$, and then with probability one, there exist \mathbf{z} such that $f^*(\mathbf{x}) - f^*(\mathbf{z}) = \|\mathbf{x} - \mathbf{z}\|$ and both points are different $\mathbf{x} \neq \mathbf{z}$. For each $t \in [0, 1]$ let $\mathbf{x}_t = (1 - t)\mathbf{x} + t\mathbf{z}$ and the path $\sigma : [0, 1] \rightarrow \mathbb{R}$ defined as $\sigma(t) := f^*(\mathbf{x}_t) - f^*(\mathbf{x})$. The proof is split in two steps;

Step 1 ($\sigma(t) = \|\mathbf{x}_t - \mathbf{z}\| = t\|\mathbf{x} - \mathbf{z}\|$)

First of all we realize that for each $s, t \in [0, 1]$

$$|\sigma(t) - \sigma(s)| = |f^*(\mathbf{x}) - f^*(\mathbf{x}_s)| \leq \|\mathbf{x}_t - \mathbf{x}_s\| \leq |t - s|\|\mathbf{x} - \mathbf{z}\|.$$

Actually if we consider $t \in [0, 1]$ then

$$\begin{aligned} \sigma(1) - \sigma(0) &\leq \sigma(1) - \sigma(t) + \sigma(t) - \sigma(0) \\ &\leq (1 - t)\|\mathbf{x} - \mathbf{z}\| + \sigma(t) - \sigma(0) \\ &\leq (1 - t)\|\mathbf{x} - \mathbf{z}\| + t\|\mathbf{x} - \mathbf{z}\| = \|\mathbf{x} - \mathbf{z}\| = \sigma(1) - \sigma(0) \end{aligned}$$

And the inequalities become equalities and because $\sigma(0) = 0$ we conclude $\sigma(t) = t\|\mathbf{x} - \mathbf{z}\|$.

Step 2 (There exists some unitary vector \mathbf{v} such that $|(\partial f^*/\partial \mathbf{v})(\mathbf{x})| = 1$)

The candidate is $\mathbf{v} = \frac{\mathbf{z} - \mathbf{x}}{\|\mathbf{z} - \mathbf{x}\|}$, and lets compute the partial derivative

$$\begin{aligned} \frac{\partial f^*}{\partial \mathbf{v}}(\mathbf{x}) &= \lim_{h \rightarrow 0} \frac{f(\mathbf{x} + h\mathbf{v}) - f(\mathbf{x})}{h} \\ &= \lim_{h \rightarrow 0} \frac{\sigma\left(\frac{h}{\|\mathbf{z} - \mathbf{x}\|}\right)}{h} = 1. \end{aligned}$$

Then for each differentiable point x of f^* there exists an unitary vector \mathbf{v} such that $|\partial f^*/\partial \mathbf{v}(\mathbf{x})| = 1$. Then by creating an orthonormal base such that \mathbf{v} belongs to it we can deduce that $\|\nabla f^*(\mathbf{x})\| = 1$. And this event occurs with almost surely because of Rademacher Theorem.

C Lipshitz constant for convolutional networks

C.1 Enforcing 1-Lipschitz dense layer

A neural network is a composition of linear and non-linear function. Let's study first a multilayer perceptron is defined as follows :

$$f(x) = \phi_k(W_k \cdot (\phi_{k-1}(W_{k-1} \dots \phi_1(W_1 \cdot x))).$$

We name $L(f)$ the Lipschitz constant of a function f . As a composition of functions, the Lipschitz constant of a multilayer perceptron is upper bounded by the product of the individual Lipschitz constants:

$$L(f) \leq L(\phi_k) * L(W_k) * L(\phi_{k-1}) * L(W_{k-1}) * \dots * L(\phi_1) * L(W_1 \cdot x).$$

The most common activation functions such as ReLU or sigmoid are 1-Lipschitz. Thus, we can ensure that a perceptron is 1-Lipschitz by ensuring each dense layer W_k is 1-Lipschitz. Given a linear function represented by an $n \times m$ matrix W , it is commonly admitted that:

$$L(W) = \|W\| \leq \|W\|_F \leq \max_{ij}(|W_{ij}|) * \sqrt{nm} \quad (33)$$

where $\|W\|$ is the spectral norm, and $\|W\|_F$ is the Frobenius norm. The initial version of WGAN [2] clip the weights of the networks. However, this is a very crude way to upper-bound the 1-Lipschitz (see equation 33). Normalizing by the Frobenius norm have also been proposed in [25]. In this paper, we use spectral normalization as proposed in [19]. At the inference step, we normalize the weights of each layer by dividing the weight by the spectral norm of the matrix:

$$W_s = \frac{W}{\|W\|}.$$

Even if this method is more computationally expensive than Frobenius normalization, it gives a finer upper bound of the 1-Lipschitz constraint of the layer. The spectral norm is computed by iteratively evaluating the largest singular value with the power iteration algorithm [11]. This is done during the forward step and taken into account for the gradient computation.

C.2 Enforcing 1-Lipschitz convolutional layer

In this section we will show that enforcing convolution kernels to 1-lispchitz is not enough for ensuring the 1-lipschitz property of convolutional layers, and will propose two normalization factors. Notations: We consider a Convolutional layer with an input feature map X of size (c, w, h) , and L output channels obtained with kernels $W = \{W_l\}_{l \in [0, L]}$ of odd size (c, k, k) , i.e. $k = 2 * \bar{k} + 1$. Considering the classical *same* configuration which output size is (L, w, h) , we use the following matrix notations of the convolution $Y = W * X$:

- \tilde{X} the zero padded matrix of X of size $(c, w + k - 1, h + k - 1)$
- \bar{W} the vectorized matrix of weights of size $(L, c \cdot k^2)$
- \bar{X} a matrix of size $(c \cdot k^2, w \cdot h)$, a duplication of the input \tilde{X} , where each column j correspond to the $c \cdot k^2$ inputs in \tilde{X} used for computing a given output j
- $\bar{Y} = \bar{W} \cdot \bar{X}$ the vectorized output of size $(L, w \cdot h)$

Given two outputs X_1 and X_2 , we can compute an upper bound of convolutional layer lipschitz constant (Eq. 34).

$$\begin{aligned} \|Y_1 - Y_2\|^2 &= \|\bar{Y}_1 - \bar{Y}_2\|^2 \leq \|\bar{W}\|^2 \cdot \|\bar{X}_1 - \bar{X}_2\|^2 \\ &\leq \Lambda^2 \cdot \|W\|^2 \cdot \|X_1 - X_2\|^2 \end{aligned} \quad (34)$$

The coefficient Λ^2 can be estimated, as in [6], by the maximum number of duplication of the input matrix \tilde{X} in \bar{X} : each input can be used at most in k^2 positions. But since within \bar{X} , part of the

values come from the zero padded zones in \tilde{X} , and have no influence on $\|Y_1 - Y_2\|^2$, we propose a tighter estimation of Λ , computing the average duplication factor of non zero padded value in \tilde{X} .

For a 1D convolution (see Fig. 6), the number of zero values in the \bar{k} first columns of \tilde{X} (symmetrically on the \bar{k} last columns) is $(\bar{k}, \bar{k} - 1, \dots, 1)$. So the number of zero padded values is $k.w - 2 * \sum_{t=1}^{\bar{k}} t = k.w - \bar{k}(\bar{k} + 1)$.

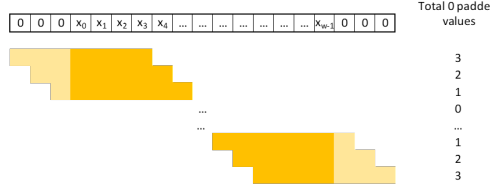


Figure 6: Zero padded elements in a 1D convolution with $k = 7$ ($\bar{k} = 3$)

We propose to use Eq. 35 as a tighter normalization factor³.

$$\Lambda = \sqrt{\frac{(k.w - \bar{k}(\bar{k} + 1)).(k.h - \bar{k}(\bar{k} + 1))}{h.w}} \quad (35)$$

C.3 Convolution layers with zero padding and stride

Convolution layers are sometimes used with stride (as in Resnet layers [14]) to reduce the computation cost of these layers⁴. Given a stride (s, s) , the output layer size of the layer will be (wo, ho) such as $w = s.wo + rw$ and $h = s.ho + rh$. We also introduce $\alpha = \lceil \frac{k}{s} \rceil$ the maximum number of overlapping stride positions. As in previous section, we can build a matrix \tilde{X} of size $(c.k^2, wo.ho)$, as a duplication of \tilde{X} . The maximum duplication factor of an element of \tilde{X} in \tilde{X} is $\Lambda^2 = \alpha^2$.

As in section C.2, we can compute a tighter factor using the average duplication factor of input in X , by computing the number of non-zero-padded values used in \tilde{X} . We introduce $\bar{\alpha}, \bar{\beta}$ such as $\bar{k} = \bar{\alpha}.s + \bar{\beta}$.

For a 1D convolution (see Fig. 7), the number of zero values in the first columns of \tilde{X} is $(\bar{k}, \bar{k} - s, \dots, \bar{\beta})$. So the number of zero padded values on the left side is $zl = \sum_{t=0}^{\bar{\alpha}} (\bar{k} - t.s) = (\bar{\alpha} + 1)\bar{k} - s \cdot \frac{\bar{\alpha}(\bar{\alpha}+1)}{2} = \frac{(\bar{\alpha}+1)(\bar{\alpha}s+2\bar{\beta})}{2}$.

On the right side (last columns), we introduce $\gamma_w = \text{argmax}\{\gamma = w - 1 - i.s, \text{ such as } i \geq 0 \text{ and } \gamma \leq \bar{k}\}$ i.e. $\gamma_w = w - 1 - s \lceil \frac{w-1-\bar{k}}{s} \rceil$. γ_w represents the first half-kernel to include the last element of the line. We also introduce α_w, β_w such as $\gamma_w = \alpha_w.s + \beta_w$. The number of zero values in the last columns is $(\bar{k} - \gamma_w, \bar{k} - \gamma_w + s, \dots, \bar{k} - \gamma_w + \alpha_w.s)$, i.e. $zr_w = \sum_{t=0}^{\alpha_w} (\bar{k} - \gamma_w + t.s) = (\alpha_w + 1)(\bar{k} - \gamma_w + \frac{s.\alpha_w}{2})$.

For the matrix \tilde{Y} the average duplication factor for a value of the input X is $\frac{(k.wo - zl - zr_w).(k.ho - zl - zr_h)}{h.w}$

We propose to use Eq. 36 as a tighter normalization factor⁵⁶.

$$\Lambda = \sqrt{\frac{(k.wo - zl - zr_w).(k.ho - zl - zr_h)}{h.w}} \quad (36)$$

³this factor Eq. 35 is not a strict upper bound of the lipschitz constant, since particular matrix with high value on the center and low values on borders won't satisfy the inequality (34)

⁴main drawback with stride is that each point in the input feature map has not the same number of occurrences

⁵As in previous section, this factor is not an upper bound of the lipschitz constant

⁶in case of stride $s = 1$, we have $\bar{\alpha} = \bar{k}$, $\bar{\beta} = 0$, $\gamma_w = \alpha_w = \bar{k}$ and $\beta_w = 0$. So we can retrieve $zl + zr_w = \frac{\bar{k}(\bar{k}+1)}{2} + \frac{\bar{k}(\bar{k}+1)}{2} = \bar{k}(\bar{k} + 1)$

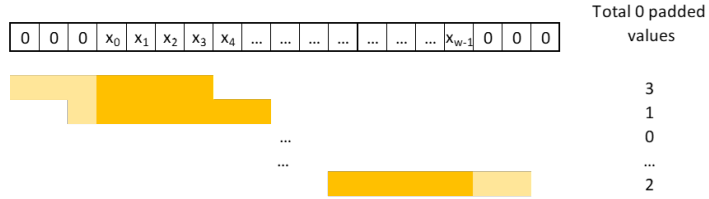


Figure 7: Zero padded elements in a 1D convolution with stride: $k = 7$ ($\bar{k} = 3$), and $s = 2$

Layer type	Parameters	Upper lip constant	Thighter Lip estimation
Dense		$\ W\ $	
Convolution wo stride	kernel size (k, k) $k = 2\bar{k} + 1$	$k \cdot \ W\ $	$\sqrt{\frac{(k \cdot w - \bar{k} \cdot (\bar{k} + 1)) \cdot (k \cdot h - \bar{k} \cdot (\bar{k} + 1))}{h \cdot w}} \cdot \ W\ $
Convolution with stride	kernel size (k, k) stride (s, s)	$\lceil \frac{k}{s} \rceil \cdot \ W\ $	$\sqrt{\frac{(k \cdot wo - zl - zr_w) \cdot (k \cdot ho - zl - zr_h)}{h \cdot w}} \cdot \ W\ $
MaxPoolig		1	
AveragePooling	averaging size po stride s	$\lceil \frac{po}{s} \rceil \cdot \frac{1}{po}$	

Table 2: Main

C.3.1 Pooling layers

By definition, the max pooling layer is 1-lipschitz, since $\|max(X_1) - max(X_2)\| \leq \|X_1 - X_2\|$ [28].

Considering average pooling layer with a averaging size of po , and a stride of s . Since a mean is equivalent to a convolution with the matrix $\frac{1}{po^2} \mathbb{1}_{po \times po}$. The average pooling layer is equivalent to a convolution with stride (sec C.3). Introducing $\alpha = \lceil \frac{po}{s} \rceil$, which is 1 in the common case where $s = po$. So an upper bound of lipschitz constant for the average pooling layer is $\Lambda \cdot \|W\| = \frac{\alpha}{po}$

C.4 Gradient norm preserving and general architecture

As proven Sections 3.2 and , the optimal function f^* with respect to Equation 5, verifies $\|\nabla f^*\| = 1$ almost surely. In [13], the authors propose to add a regularization terms with respect to the average gradient norm with respect to inputs in the loss function. However, the estimation of this value is difficult and a regularization term doesn't guarantee the property. In this paper, we apply the approach described in [1], based on the use of specific activation functions and a normalization process of the weights. Three norm preserving activation functions are proposed:

- **MaxMin** : order the vector by pairs.
- **GroupSort** : order the vector by group of a fixed size.
- **FullSort** : order the vector.

These function are vector-wise rather than element-wise. We also propose the activation **Const-PReLU**, a PReLU [15] activation function complemented by a constraint such that $|\alpha| \leq 1$ (α the learnt slope). This last function is norm preserving only when $|\alpha| = 1$ (linear, or absolute value function), but being computed element wise, it is then more efficient for convolutional layers outputs.

Given a vector v of size k the P-norm pooling is defined in [4] as follows :

$$Pool_{P-norm}(v) = \left(\frac{1}{k} \sum_{i=1}^k v_i^p P \right)^{\frac{1}{p}}$$

Concerning linear functions, a weight matrix W is norm preserving if and only if all the singular values of W are equals to 1. In [1], the authors propose to use the Björk Orthonormalization algorithm [3]. The Björk algorithm compute the closest orthonormal matrix by repeating the following operation :

$$W_{k+1} = W_k \left(I + \sum_{i=1}^p (-1)^p \begin{pmatrix} -\frac{1}{2} \\ p \end{pmatrix} Q_k^p \right) \quad (37)$$

where $Q_k = 1 - W_k^T W_k$ and $W_0 = W$. This algorithm is fully differential, and as for spectral normalization, it is applied during the forward inference, and taken into account for back-propagation.

D Experiments : additional results

D.1 Networks architecture

We apply these normalization both to dense and convolutional layers. All the weights are initialized with Björk algorithm with 15 steps. We consider both ReLU and norm preserving activation functions. For convolutional layers, we also apply the lipschitz coefficients correction (Sect. C.2) and we restrict the norm preserving activation functions to GroupSort-2, and ConstPReLU for efficiency sake⁷.

For Two-Moons dataset, the network architecture a MLP with 256-128-64-1 layer sizes. For MNIST 0-8 subset, we use respectively a MLP with 128-64-32-1 layer sizes, or a Convolutional Neural Network, using 3x3 convolution kernels, with C32-C32-P-C64-C64-C64-P-D128-D1 (the same architecture is used with sigmoid output. For Celeb-A male mustache dataset, VGG architecture is used with 3x3 convolution kernels: C16-C16-P-C32-C32-C32-P-C128-C128-C128-P-C256-C256-C256-P-D128-D64-D32-D1. For all experiments Average Pooling have shown better results than maxPooling. Other experiments were driven with ResNet networks, but leading to the same kind of results.

Lipschitz network were learnt with *DEEL.LIP*⁸ library. After the training step, the weights are replaced by their normalized version

D.2 effect of λ

The proposed regularized optimal transport for classification is applied on the two digits (0-8) MNIST subset [17], and the CelebA[18] male (with-without) mustache subset. Learning is done with the *DEEL.LIP*⁹ library, using the Hinge-KR loss (Eq. 5), varying the λ parameter, using Adam optimizer on 50 epochs, repeated 10 times, and collecting on the test dataset both the Wasserstein distance estimation, and the accuracy.

Fig. 8 shows the influence of the hyper-parameter λ introduced in eq. 5. As expected, the regularization tends to enhance the classification performance, but induce a slight drop on the Wasserstein distance estimation.

D.3 Approximating Wasserstein distance

We first consider the computation of the Wasserstein distance between two distributions using several kind of Lip_1 neural networks architectures. The architectures are inspired by [1], but the objective is slightly different, since we are not in the scope of WGAN where the generated distribution aims to decrease this distance. In our scope, the distributions are fixed, and the Wasserstein distance can be computed empirically (A.1) as a reference.

We will compare several kind of Lip_1 neural networks, Multi Layer Perceptron and Convolutional Neural Network, with spectral normalization, and Björk orthonormalization[3; 1], and activation function ReLU, constrained PReLU (sec. C.4), MaxMin, Groupsort2, FullSort [1]. Empirical Wasserstein distance is estimated using the POT library[9], applied on two digits (0-8) MNIST subset[17].

⁷others regularization layers such as BatchNorm and Dropout are useless and can modify the lipschitz factor

⁸<https://github.com/deel-ai/deel-lip> to be published soon

⁹<https://github.com/deel-ai/deel-lip> to be published soon

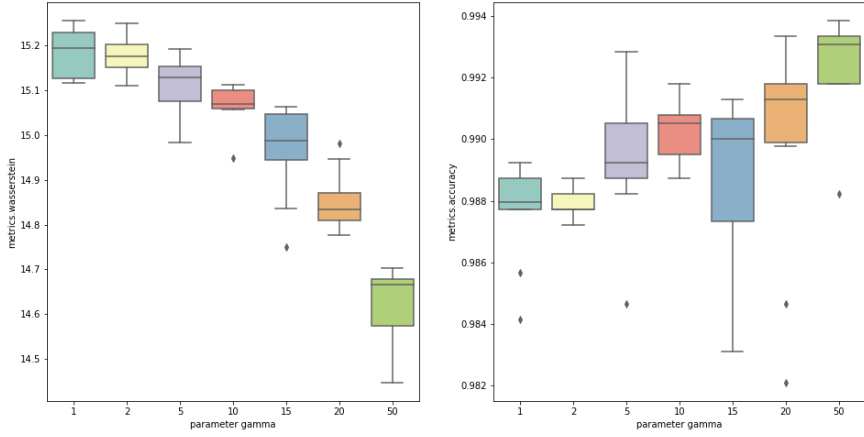


Figure 8: Influence of λ hyperparameter on regularized OT classifier (left: wasserstein distance estimation; right:classification accuracy) with a 1-lipschitz MLP on MNIST 0-8 dataset

Learning is done using the *DEEL.LIP*¹⁰ library with the wasserstein loss (Kantorovich-Rubinstein formulation), and Adam optimizer (initial learning rate 0.01) on 50 epochs. Each experiment on MNIST dataset are repeated ten times.

Results presented in table 2 show that the best approximation is obtained using MLP architecture, with Björck orthonormalization and FullSort activation. It has to be noticed that even for a simple dataset as *MNIST0 – 8*, none configuration is able to achieve the empirical Wasserstein distance value. Several possible explanations are possible: it can be due to the representativeness of the chosen *Lip*₁ Neural Network (architecture and activation) among the *Lip*₁ functions, but it could also be the consequence of an optimization problem. For the former, we use *Lip*₁ layers which gives only an upper bound for the full network lipschitz constant, but has shown in Figure3b, the overall lipschitz factor is close to one. Besides, many experiments (not presented in this paper) have been done on the size and deepness of the Neural networks with roughly the same results. For the latter, since the the orthonormalized (Björck) networks are a subclass of spectral normalization based ones, but results are worse with spectral normalization, optimization issues could be foreseen. Experiments done with many type of optimizers (Adam, SGD, RMSprop,...) lead to the same results, and surprisingly the variance of Wassertein estimations is very low (table 2).

Besides, activation functions choice has also a big influence on the Wasserstein estimation, since choosing ReLU for a MLP leads to a drop of 12% in the estimation. For Convolutional Neural Network, best results for are obtained with Björck orthonormalization and constrained PReLU activation, but are worse than MLP. This may be due to the non-invariance to shift and scale of the Wasserstein distance.

¹⁰<https://github.com/deel-ai/deel-lip> to be published soon

Dataset	Network archi	Lipschitz type	Activation	Wass estimation
TwoMoons (noise = 0.05)	[empirical estim.]	N.A.	N.A.	13.14
	MLP_1	Björck (15 it)	FullSort	13.13
	MLP_1	Björck (15 it)	GroupSort2	13.11
	MLP_1	Björck (15 it)	ReLU	12.87
	MLP_1	Spectral norm.	FullSort	12.88
MNIST 0-8	[empirical estim.]	N.A.	N.A.	19.04
	MLP_2	Björck (15 it)	FullSort	15.20 ± 0.03
	MLP_2	Björck (15 it)	GroupSort2	14.60 ± 0.08
	MLP_2	Björck (15 it)	PReLU	13.62 ± 0.03
	MLP_2	Björck (15 it)	ReLU	13.34 ± 0.07
	MLP_2	Spectral norm.	FullSort	13.18 ± 0.40
	CNN	Björck (15 it)	FullSort	11.75 ± 0.29
	CNN	Björck (15 it)	GroupSort2	11.20 ± 0.05
	CNN	Björck (15 it)	PReLU	12.30 ± 0.15
	CNN	Björck (15 it)	ReLU	11.11 ± 0.05
	CNN	Spectral norm.	FullSort	11.62 ± 0.23

Table 3: Wasserstein estimation for various dataset, and various architecture (MLP_1 : 256,128,64,1; MLP_2 : 128-64-32-1; CNN : C32-C32-P-C64-C64-C64-P-128-1)

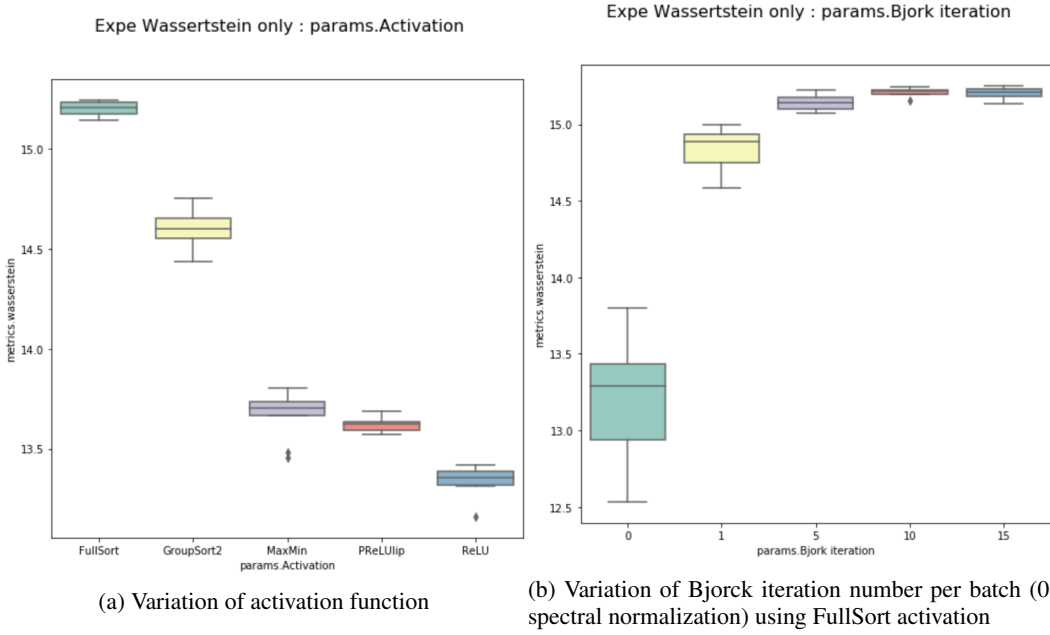


Figure 9: Estimation of Wasserstein distance with a Lipschitz MLP

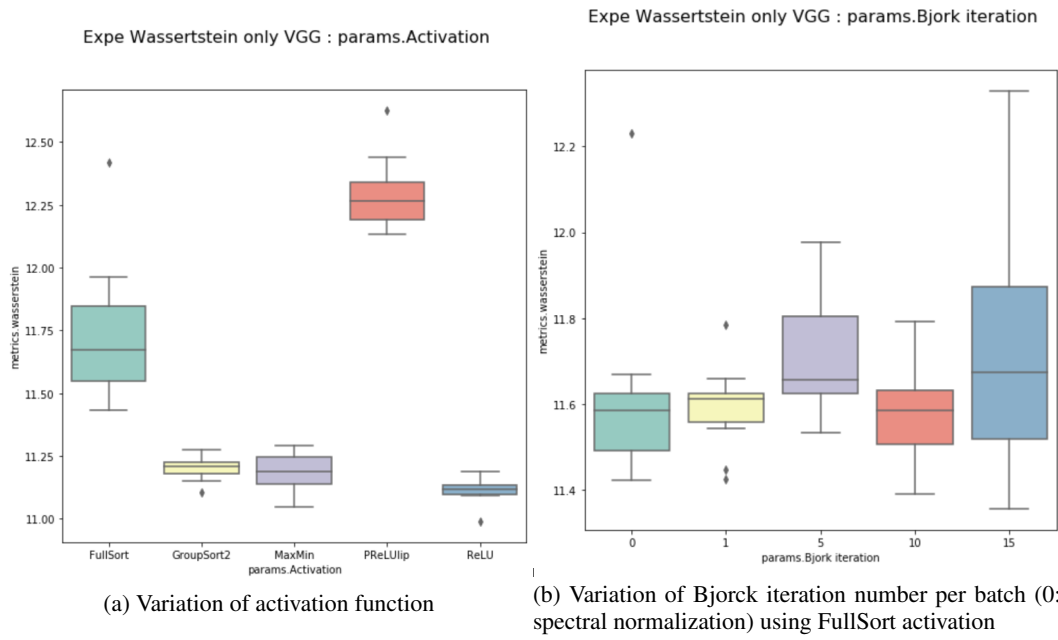


Figure 10: Estimation of Wasserstein distance with a Lipschitz Convolutional Neural Network